# S100A8/A9 drives the formation of procoagulant platelets through GPIbα

Colicchia, Martina; Schrottmaier, Waltraud C.; Perrella, Gina; Reyat, Jasmeet S.; Begum, Jenefa; Slater, Alexandre; Price, Joshua; Clark, Joanne C; Zhi, Zhaogong; Simpson, Megan; Bourne, Joshua; Poulter, Natalie S.; Khan, Abdullah Obaid; Nicolson, Phillip Lindsay Ross; Pugh, Matthew Richard; Harrison, Paul; Iqbal, Asif J; Rainger, George E.; Watson, Steve P; Thomas, Mark R.

*DOI:*
10.1182/blood.2021014966

American Society of Hematology
2021 L Street NW, Suite 900,
Washington, DC 20036
Phone: 202-776-0544 | Fax 202-776-0545
editorial@hematology.org

# S100A8/A9 drives the formation of procoagulant platelets through GPIbα

Tracking no: BLD-2021-014966R3

Martina Colicchia (1Institute of Cardiovascular Sciences, College of Medical and Dental Sciences, University of Birmingham, United Kingdom) Waltraud Schrottmaier (Medical University of Vienna, Austria) Gina Perrella (University of Birmingham, United Kingdom) Jasmeet Reyat (University of Birmingham, United Kingdom) Jenefa Begum (University of Birmingham, United Kingdom) Alexandre Slater (University of Birmingham, United Kingdom) Joshua Price (Institute of Inflammation and Ageing, United Kingdom) Joanne Clark (University of Birmingham, United Kingdom) Zhaogong Zhi (University of Birmingham, United Kingdom) Megan Simpson (University of Aberdeen, United Kingdom) Joshua Bourne (Monash University, Australia) Natalie Poulter (University of Birmingham, United Kingdom) Abdullah Khan (University of Birmingham, United Kingdom) Phillip Nicolson (University of Birmingham, United Kingdom) Matthew Pugh (University of Birmingham, United Kingdom) Paul Harrison (University of Birmingham, United Kingdom) Asif Iqbal (University of Birmingham, United Kingdom) George Rainger (The University of Birmingham, United Kingdom) Steve Watson (University of Birmingham, United Kingdom) Mark Thomas (University of Birmingham, United Kingdom) Nicola Mutch (University of Aberdeen, United Kingdom) Alice Assinger (Medical University of Vienna, Austria) Julie Rayes (University of Birmingham, United Kingdom)

**Abstract:**
S100A8/A9, also known as calprotectin or MRP8/14, is an alarmin primarily secreted by activated myeloid cells and platelets with anti-microbial, pro-inflammatory and pro-thrombotic properties. Increased plasma levels of S100A8/A9 in thrombo-inflammatory diseases are associated with thrombotic complications. We assessed the presence of S100A8/A9 in the plasma and lung autopsies from patients with COVID-19 and investigated the molecular mechanism by which S100A8/A9 affects platelet function and thrombosis.

S100A8/A9 plasma levels were increased in patients with COVID-19 and sustained high levels during hospitalization correlated with poor outcomes. Heterodimeric S100A8/A9 was mainly detected in neutrophils and deposited on the vessel wall in COVID-19 lung autopsies. Immobilization of S100A8/A9 with collagen accelerated the formation of a fibrin-rich network following perfusion of recalcified blood at venous shear. *In vitro*, platelets adhered and partially spread on S100A8/A9 leading to the formation of distinct populations of either P-selectin or phosphatidylserine-positive platelets. Using washed platelets, soluble S100A8/A9 induced phosphatidylserine exposure but failed to induce platelet aggregation, despite GPIIb/IIIa activation and alpha-granule secretion. We identified GPIbα as the receptor for S100A8/A9 on platelets inducing the formation of procoagulant platelets with a supporting role for CD36. The effect of S100A8/A9 on platelets was abolished by recombinant GPIbα ectodomain, platelets from Bernard-Soulier Syndrome patient with GPIb-IX-V deficiency and platelets from mice deficient in the extracellular domain of GPIbα.

In conclusion, we identified the S100A8/A9-GPIbα interaction as a novel targetable prothrombotic pathway inducing procoagulant platelets and fibrin formation, in particular in diseases associated with high levels of S100A8/A9, such as COVID-19.

**Conflict of interest:** COI declared - see note

**COI notes:** This work is protected by University of Birmingham (UoB) patent (PCT/GB2022/052007).

**Preprint server:** No;

**Author contributions and disclosures**: MC designed and performed experiments, collected and analyzed data and wrote the manuscript; WCS, GP, MJS, JP, JCC, JB, JSR, ZZ, AS performed experiments and analyzed data; JHB and AOK analyzed data; MP, NSP; PLRN, PH, AJI, GER, SPW and MRT provided key reagents and contributed to data analysis; NJM and AA provided key reagents and supported research design and analysis; JR designed research and experiments, performed experiments, collected and analyzed data and wrote the manuscript. All authors read and approved the paper.

**Non-author contributions and disclosures**: No;

**Agreement to Share Publication-Related Data and Data Sharing Statement**: N/A

**Clinical trial registration information (if any)**:

# S100A8/A9 drives the formation of procoagulant platelets through GPIbα

Martina Colicchia[1], Waltraud C. Schrottmaier[2], Gina Perrella[1,3], Jasmeet S. Reyat[1], Jenefa Begum[1], Alexandre Slater[1], Joshua Price[4], Joanne C. Clark[1], Zhaogong Zhi[1], Megan J. Simpson[5], Joshua H. Bourne[1], Natalie S. Poulter[1,6], Abdullah O. Khan[1], Phillip L.R. Nicolson[1,7], Matthew Pugh[8], Paul Harrison[4], Asif J. Iqbal[1], George E. Rainger[1], Steve P. Watson[1,6], Mark R. Thomas[1], Nicola J. Mutch[5], Alice Assinger[2], Julie Rayes[1,6*].

[1]Institute of Cardiovascular Sciences, College of Medical and Dental Sciences, University of Birmingham, Vincent Drive, B15 2TT, Birmingham, U.K.; [2]Center for Physiology and Pharmacology, Medical University of Vienna, Vienna, Austria; [3]Dept. of Biochemistry, CARIM, Maastricht University, Maastricht (NL); [4]Institute of Inflammation and Ageing, University of Birmingham, Birmingham, U.K., [5]Aberdeen Cardiovascular & Diabetes Centre, Institute of Medical Sciences, School of Medicine, Medical Sciences and Nutrition, University of Aberdeen, Aberdeen, U.K.; [6]Centre of Membrane Proteins and Receptors (COMPARE), Universities of Birmingham and Nottingham, The Midlands, U.K., [7]Department of Haematology, Queen Elizabeth Hospital, Birmingham, B15 2TH, U.K.; [8]Institute of Immunology and Immunotherapy, University of Birmingham, Birmingham, B15 2TT, U.K.

*Corresponding author: Dr Julie Rayes, J.Rayes@bham.ac.uk

Running title: S100A8/A9-GPIbα interaction drives thrombosis.

Key words: S100A8/A9, calprotectin, fibrin, procoagulant platelets, GPIbα

Word count: 4100

## Key Points

**Main Point 1**: S100A8/A9 plasma levels are increased in patients with COVID-19 and sustained high levels are associated with worse clinical outcome.

**Main point 2**: S100A8/A9 induces the formation of procoagulant platelets through GPIbα supporting fibrin generation and immune-driven thrombosis.



## Abstract

S100A8/A9, also known as calprotectin or MRP8/14, is an alarmin primarily secreted by activated myeloid cells and platelets with anti-microbial, pro-inflammatory and pro-thrombotic properties. Increased plasma levels of S100A8/A9 in thrombo-inflammatory diseases are associated with thrombotic complications. We assessed the presence of S100A8/A9 in the plasma and lung autopsies from patients with COVID-19 and investigated the molecular mechanism by which S100A8/A9 affects platelet function and thrombosis.

S100A8/A9 plasma levels were increased in patients with COVID-19 and sustained high levels during hospitalization correlated with poor outcomes. Heterodimeric S100A8/A9 was mainly detected in neutrophils and deposited on the vessel wall in COVID-19 lung autopsies. Immobilization of S100A8/A9 with collagen accelerated the formation of a fibrin-rich network following perfusion of recalcified blood at venous shear. *In vitro*, platelets adhered and partially spread on S100A8/A9 leading to the formation of distinct populations of either P-selectin or phosphatidylserine-positive platelets. Using washed platelets, soluble S100A8/A9 induced phosphatidylserine exposure but failed to induce platelet aggregation, despite GPIIb/IIIa activation and alpha-granule secretion. We identified GPIbα as the receptor for S100A8/A9 on platelets inducing the formation of procoagulant platelets with a supporting role for CD36. The effect of S100A8/A9 on platelets was abolished by recombinant GPIbα ectodomain, platelets from Bernard-Soulier Syndrome patient with GPIb-IX-V deficiency and platelets from mice deficient in the extracellular domain of GPIbα.

In conclusion, we identified the S100A8/A9-GPIbα interaction as a novel targetable prothrombotic pathway inducing procoagulant platelets and fibrin formation, in particular in diseases associated with high levels of S100A8/A9, such as COVID-19.

## INTRODUCTION

Platelets are crucial for hemostasis and are key drivers of pathogenic thrombosis both in sterile and infectious conditions[1,2]. Circulating activated platelets and platelet-leukocyte aggregates are increased in acute and chronic sterile thrombo-inflammatory diseases such as atherosclerosis[3], deep vein thrombosis (DVT)[4], ischemic stroke[5] and myocardial infarction (MI)[6,7] and in infectious conditions such as sepsis[8], influenza[9] and in COVID-19[10] with the increase in these levels correlating with disease severity[11–13]. Moreover, procoagulant platelets and microvesicles (MVs), which support fibrin generation independent of platelet aggregation, are observed in trauma[14], COVID-19[15], coronary artery disease[16,17], sepsis[18,19], DVT and stroke[20–22] but the mechanism triggering their formation is not well understood.

Activation of neutrophils and neutrophil extracellular traps formation (NETosis) lead to the release of damage-associated molecular patterns (DAMPs) such as histones, myeloperoxidase (MPO) and S100A8/A9, which can promote inflammation and thrombosis[23,24]. Recent work has demonstrated that plasma levels of S100A8/A9, also known as calprotectin or MRP-8/MRP-14, are elevated in patients with COVID-19 and correlate with disease severity as well as thrombotic complications[25–29]. High S100A8/A9 levels are also observed in myocardial infarction[30–32], sepsis[33] and DVT[34] with S100A8/A9 being proposed as a biomarker for immune cell activation and inflammation[35–37]. S100A8 and S100A9 proteins belong to the 24 members of the multifunctional S100 family of cytoplasmic EF-hand helix-loop-helix $Ca^{2+}$-binding proteins regulating $Ca^{2+}$ balance, cell apoptosis, migration, proliferation, differentiation, energy metabolism and inflammation[38]. Extracellular S100A8 and S100A9 and the heterodimer S100A8/A9 promote inflammation and endothelial activation[39]. The heterodimer S100A8/A9 is the predominant form, comprising up to 45% and ~5% of all cytosolic proteins in neutrophils as well as monocyte/macrophages, respectively[38,40,41]. Three receptors have been described to mediate S100A8/A9 proinflammatory functions: the receptor for advanced glycation end products (RAGE), toll-like receptor-4 (TLR4) and the scavenger receptor CD36, which are expressed on different cells including platelets, immune cells and endothelial cells[42–45]. Innate immune cell activation leads to the release of S100A8/A9 and its deposition on venules, supporting leukocyte recruitment and transmigration[29]. Moreover, binding of S100A8/A9 to endothelial cells promotes their activation, through heparan sulfate glycosaminoglycans[46], CD36[47] and RAGE[39]. Therefore, both soluble and immobilized S100A8/A9 may contribute to inflammation and thrombosis[27,34], with multiple receptors and mechanisms involved in thrombo-inflammatory diseases. Here, we investigated the function of extracellular S100A8/A9 as a DAMP regulating platelet function and thrombosis. We show that S100A8/A9 induces procoagulant platelets through GPIbα, independently of the known receptors for S100A8/A9, TLR4 and RAGE. CD36 blockage partially reduced GPIIb/IIIa activation and phosphatidylserine exposure on platelets without alteration in P-selectin expression. We have identified the S100A8/A9-GPIbα interaction as a novel prothrombotic pathway which triggers the formation of procoagulant platelets accelerating fibrin generation and thrombosis.

## MATERIALS AND METHODS

### Ethical approval

Ethical approval for collecting blood from healthy volunteers was granted by Birmingham University Internal Ethical Review (ERN_11-0175). Mouse experiments were performed in accordance with UK laws (Animal [Scientific Procedures] Act 1986) with approval of the local ethical committee and UK Home Office approval (PPL Pp9677279). Ethical approval for collecting post-mortem tissues was granted by the North-East - Newcastle & North Tyneside 1 Research Ethics Committee, (19/NE/0336). Collection of post-mortem formalin-fixed and paraffin-embedded tissue was approved (IRAS: 197937) for tissue obtained via prospective consent post-mortem and retrospective acquisition of tissue in which consent for use in research had already been obtained. Ethics for patient tissue were approved by the Health Research Authority (HRA) with an NHS (National Health Service) REC (Research Ethics Committee); All necessary patient/participant written consent has been obtained and the appropriate institutional forms have been archived. This research adheres to the tenets of the Declaration of Helsinki. Blood from patients with COVID-19 was collected under the ethical approval of Medical University of Vienna (EK1315/2020) as part of the Austrian Coronavirus Adaptive Clinical Trial (ACOVACT; ClinicalTrials.gov NCT04351724).

### Plasma S100A8/A9 ELISA

Plasma was collected by blood centrifugation for 10 min at 1000 x g (4 °C) followed by 10 min centrifugation at 10.000 x g at room temperature (RT)[48]. Plasma samples were stored at -80 °C until use. Plasma levels of S100A8/A9 were measured using LEGEND MAX Human MRP8/14 (Calprotectin) ELISA Kit (BioLegend).

### Immunofluorescence staining of lung sections

Human paraffin embedded lung sections (6 µm) were processed and stained as previously described[49]. Antibodies against platelet CD42b, MPO, fibrin, S100A8/A9 and S100A9 (Supplementary Table 1) were incubated overnight at 4 °C followed by secondary conjugated antibodies. Lung autofluorescence was quenched using commercial kit (Vector laboratories) and slides mounted using ProLong Gold Antifade Mountant (Life Technologies). Sections were imaged using an Epifluorescent microscope or Zeiss Axioscan Z1 microscope and analyzed using ZEN software and image J.

### Recombinant S100A8/A9 production and purification

Commercial recombinant S100A8/A9 (BioLegend) and *in-house* produced proteins were used. Recombinant human heterodimeric S100A8/A9 was produced as previously described with minor changes[50]. Protein production and purification is detailed in supplemental data.

### Platelet preparation and functional assays

Human and mouse blood was collected in sodium citrate and ACD-A Anticoagulant Citrate Dextrose solution, respectively, as previously described[51,52]. Platelet preparation and functional assays (platelet aggregation and ATP generation, thrombin generation test, flow adhesion assay, platelet spreading, intracellular $Ca^{2+}$ release) are detailed in supplemental data.

### Data analysis

All data were presented as mean ± standard deviation (SD) unless stated otherwise. The logarithmic dose-binding curves were generated through four-parameter nonlinear regression analysis with variable slopes. The statistical difference between groups was analyzed using either a One-Way ANOVA with multiple comparisons or Kruskal-Wallis Test with multiple comparisons or as stated in figure legends using Prism 7 (GraphPad Software Inc).

## RESULTS

### Sustained high levels of S100A8/A9 in the plasma of patients with COVID-19 correlate with adverse outcome

Plasma S100A8/A9 levels are elevated in patients with COVID-19 and these levels correlate with thrombosis[28,53,54]. In a cohort of 87 patients with COVID-19[55,56], plasma levels of S100A8/A9 were measured by ELISA over the first week of study enrolment. Study inclusion occurred up to 72 hours after hospital admission. Patients were stratified based on the clinical severity into uncomplicated (not requiring intensive care treatment) and complicated (intensive care unit [ICU] survivors and non-survivors). At study recruitment, the levels of S100A8/A9 were elevated in the plasma of all patients with COVID-19 compared to healthy controls (Figure 1A). Over the first 7 days of monitoring, the levels of S100A8/A9 remained high in patients with complicated COVID-19 but decreased in uncomplicated patients (Figure 1B, C). The levels of S100A8/A9 were significantly higher in non-survivors ranging between 10 and 40 µg/ml. These data show that sustained high levels of plasma S100A8/A9 correlated with COVID-19 disease severity.

### Heterodimeric S100A8/A9 is detected in neutrophils and on the lung vessel walls of patients with COVID-19

S100A8/A9 release from activated immune cells leads to deposition on venule endothelial cells, supporting leukocyte recruitment and transmigration[29]. The presence and location of S100A8/A9 were assessed in lung autopsies from COVID-19 non-survivor patients (n=8)[49]

and control sections from aged-matched patients (n=3). Using an antibody recognizing the heterodimer S100A8/A9 but not S100A8 or S100A9 alone, S100A8/A9 was detected in neutrophils (MPO-positive cells) and on the vessel wall (Figure 1D, E). S100A8/A9 was also detected in a fraction of CD42b-positive cells in patients with COVID-19 but not in controls. Platelets were observed lining the endothelium as single platelets, small aggregates positive for S100A9 and fibrin or integrated into large fibrin-rich thrombi (Figure 1D, F, G). Contrary to the antibody recognizing the dimeric form, staining with anti-S100A9 antibody revealed a strong colocalization between CD42b and S100A9 (Figure 1G). These results show that both S100A8/A9 plasma levels and deposition on the vasculature are observed in COVID-19 lungs.

**Immobilized S100A8/A9 supports fibrin generation at venous shear**

Platelet-derived S100A8/A9 was shown to promote endothelial cell activation and thrombosis via CD36[28,27] but the effect of S100A8/A9 on platelets is not well known. We assessed the effect of soluble and immobilized recombinant S100A8/A9 on fibrin generation in whole blood from healthy donors. Commercial and *in-house* produced recombinant S100A8/A9 were used and characterized (Supplementary Figure 1A-D). Both proteins are heterodimers and the S100A9 protein phosphorylated at Thr113, which is essential for the proinflammatory functions of extracellular S100A8/A9[57] (Supplementary Figure 1A-D). S100A8/A9 induces the secretion of TNF-α from human monocytes in a TLR4-dependent manner as TAK-242 significantly reduced TNF-α levels in monocyte supernatant, showing the functionality of *in-house* produced S100A8/A9 (Supplementary Figure 1E). Addition of S100A8/A9 in platelet rich plasma (PRP) isolated from healthy donors did not support thrombin generation in calibrated automated thrombography (CAT) compared to PRP alone (Supplementary Figure 2A-F). However, perfusion of whole blood under recalcified conditions at venous shear ($100s^{-1}$) over S100A8/A9-coated surfaces induced platelet adhesion with local fibrin generation as assessed using anti-fibrin/fibrinogen antibody and early recruitment of PS-positive platelets assessed using Annexin-V binding (Figure 1H-J). Compared to S100A8/A9 or collagen alone, surfaces coated with S100A8/A9 in combination with collagen accelerated the recruitment of Annexin-V-positive platelets and the formation of multiple fibrin-rich areas and widespread fibrin network, which significantly limited blood flow (Figure 1H-J). These results indicate that immobilized S100A8/A9 accelerates the formation of fibrin-rich thrombi at venous shear.

**Recombinant S100A8/A9 induces non-classical human platelet activation without aggregation *in vitro***

It has been recently shown that arterial and venous thrombus formation was reduced in mice deficient in S100A8/A9[27,34]. In order to identify whether S100A8/A9 exerts a direct effect on platelets leading to pathogenic thrombosis, we assessed the effect of

recombinant S100A8/A9 on platelet function *in vitro*. The incubation of human washed platelets with increasing concentrations of S100A8/A9 at ranges previously detected in thrombo-inflammatory diseases and COVID-19 patients[26,33,53,58,59] induced platelet activation as assessed by flow cytometry (Figure 2). S100A8/A9 induced a slow release of P-selectin from alpha-granule as measured using an anti-P-selectin antibody (Figure 2A, B, Supplementary Figure 2G). Platelet activation by S100A8/A9 was not homogenous among healthy donors, with high responders reaching similar levels of platelet activation as CRP and TRAP-6, even at low doses of S100A8/A9 (20µg/ml) (Figure 2B). The upregulation in P-selectin expression was associated with increased platelet-neutrophil aggregates in diluted whole blood following stimulation with S100A8/A9 (Figure 2C). S100A8/A9 induced GPIIb/IIIa activation as assessed by the binding of an anti-CD61/CD41 PAC-1 antibody which recognizes the activated form of the integrin (Figure 2D). GPIIb/IIIa activation occurred quickly following the addition of S100A8/A9 compared to the slow upregulation of P-selectin (Supplementary Figure 2H). Surprisingly, despite GPIIb/IIIa activation, S100A8/A9 did not induce platelet aggregation (Figure 2E, F) as assessed by light transmission aggregometry or dense granule release (Figure 2G, H). S100A8/A9 did not induce platelet aggregation in the presence of exogenous fibrinogen, suggesting that the absence of aggregation is not due to a defect in fibrinogen secretion (Figure 2I, J). Similarly, addition of exogenous labelled fibrinogen to platelets in the presence of S100A8/A9 showed low binding capacity compared to CRP (Figure 2K, L). These results indicate that S100A8/A9 induces P-selectin upregulation and GPIIb/IIIa activation without platelet aggregation, suggesting a novel mechanism of platelet activation independent of platelet aggregation.

## S100A8/A9 induces PS exposure on platelets and the release PS-positive microvesicles

Procoagulant platelets, which expose high levels of PS, have a very low capacity to aggregate with some procoagulant platelet populations sustaining the active form of GPIIb/IIIa[60]. Therefore, surface expression of PS on S100A8/A9-activated platelets was assessed by Annexin-V binding using flow cytometry. S100A8/A9 induced PS exposure on the surface of platelets (Figure 3A-C), which occurred rapidly following the addition of S100A8/A9 (Supplementary Figure 2I). S100A8/A9 also increased the level of PS on CD41-positive microvesicles (MV) (Figure 3D). Platelet activation is dependent on the presence of the heterodimer as recombinant S100A8 or S100A9 alone did not induce platelet activation (Supplementary Figure 2J-L). Platelets adhered to and spread on immobilized S100A8/A9, while no significant platelet adhesion was observed on BSA used as negative control (Figure 3E). Platelet adhesion on immobilized S100A8/A9 showed predominantly the selective expression of either PS or P-selectin on adherent platelets, with minimal expression of both markers in single platelets (Figure 3F, G). Increasing the coating density of S100A8/A9 augmented the formation of PS-positive platelet and PS-positive MVs rather than P-selectin positive platelets (Figure 3G). In addition, platelet

adhesion on S100A8/A9 induced intracellular $Ca^{2+}$ release (Figure 3H, I), with high $Ca^{2+}$ signals observed in adherent but not spread platelets. These results indicate that S100A8/A9 induces intracellular $Ca^{2+}$ release, PS exposure and the release of PS-positive MVs, and this activation is restricted to the heterodimeric form of S100A8/A9.

## CD36 blockade and ITAM receptor inhibitors differentially reduce the effect of S100A8/A9 on platelets

S100A8/A9 has three known receptors: RAGE, TLR4 and CD36, which are all expressed on platelets[61–63]. In order to identify the functional receptor for S100A8/A9 mediating the formation of procoagulant and activated platelets, we first assessed the effect of inhibitors targeting TLR4, RAGE and CD36 in human washed platelets. Inhibition of RAGE using Paquinimod or Azeliragon did not alter platelet activation by S100A8/A9 (Figure 4A-C). Inhibition of TLR-4, using the small molecule inhibitor TAK-242 or an antibody inhibiting S100A8/A9 binding to TLR4 and RAGE (S100A8/A9 Ab), also did not alter platelet activation or PS exposure (Supplementary Figure 3A-C, Supplementary Table 2). Blocking downstream signaling of CD36 using Sulfosuccinimidyl Oleate (SSO), which irreversibly blocks CD36, partially reduced GPIIb/IIIa activation and PS exposure without affecting P-selectin expression (Figure 4D-F). An antibody that blocks the oxidized low-density lipoprotein (Ox-LDL) binding site to CD36 (CD36 blocking Ab) had no effect on platelet activation suggesting the presence of distinct binding sites for S100A8/A9 and Ox-LDL on CD36 (Supplementary Figure 3D, E). Further, inhibition of platelet immunoreceptor tyrosine-based activation motif (ITAM) receptors using inhibitors for Src (PP2), Syk (PRT-060318) or Btk (ibrutinib) did not alter the binding of anti-CD61/CD41 PAC-1 antibody or Annexin-V (Figure 4G-I) while significantly reduced P-selectin expression on platelets (Figure 4H). Inhibition of Syk showed the highest inhibition of P-selectin expression which was associated with a decrease in platelet-neutrophil aggregates in whole blood (Supplementary Figure 3F). Inhibition of COX-1 using indomethacin or P2Y12 using cangrelor did not alter platelet activation or PS exposure (Supplementary Figure 3G-I). These results suggest that S100A8/A9-mediated P-selectin upregulation is regulated by Syk/Src while GPIIb/IIIa activation and PS exposure are partially mediated through CD36.

## Murine recombinant S100A8/A9 activates mouse platelets in a dose-dependent manner through GPIbα

As CLEC-2, GPVI, GPIb and CD36 signal through Syk/Src[64,65], we assessed the effect of S100A8/A9 on murine platelets deficient in CLEC-2, GPVI, CLEC-2/GPVI or platelets deficient in the extracellular domain of GPIbα (IL4R/GPIbα−Tg mice). Mouse S100A8/A9 induced the activation of WT platelets in a dose-dependent manner as assessed using anti-P-selectin antibody and Annexin-V binding in a similar manner as in human platelets (Figure 5A, B). Deletion of GPVI, CLEC-2 or both receptors did not significantly alter P-

selectin expression or Annexin-V binding in response to S100A8/A9 compared to WT mice (Figure 5C, D). However, GPVI$^{-/-}$ and GPVI$^{-/-}$ CLEC-2$^{-/-}$ mice showed a bimodal pattern for P-selectin expression. S100A8/A9-induced mouse platelet activation was significantly reduced in platelets deficient in the extracellular domain of GPIbα (IL4R/GPIbα−Tg) as measured by P-selectin expression (Figure 5E, F), Annexin-V binding (Figure 5G, H) and GPIIb/IIIa activation (Figure 5I, J). Compared to GPIIb/IIIa activation in human platelets, mouse S100A8/A9 induced modest integrin activation (Figure 5I, J). The partial reduction in Annexin-V binding observed in IL4R/GPIbα−Tg platelets was completely blocked by the addition of the CD36 inhibitor SSO (Figure 5K). Collectively, these results indicate that GPIbα and CD36 are putative receptors for S100A8/A9 on mouse platelets.

## Recombinant human GPIbα binds to S100A8/A9 and potentiated von Willebrand factor (vWF)-mediated platelet agglutination

In order to assess whether GPIbα is the main receptor for S100A8/A9 on human platelets, direct binding between GPIbα and S100A8/A9 was assessed by ELISA. S100A8/A9 binds to recombinant GPIbα with an EC50 of 130±75nM (Figure 6A). Furthermore, the effect of anti-GPIbα antibodies AK2 and SZ2 and OS-1, which were previously described to block the interaction of GPIbα with vWF, on S100A8/A9-induced platelet activation was assessed as above. SZ2 and AK2 antibodies which recognize distinct epitopes on GPIbα located within the anionic/sulfated tyrosine region (Tyr276-Glu282) and in the first leucine-rich repeat (Leu36-Gln59), respectively, and OS-1 peptide which allosterically inhibits GPIbα-vWF interaction were tested at concentrations previously shown to inhibit vWF-mediated platelet agglutination[66–68] (Supplementary Figure 4A-G, Figure 6B-D). AK2 and SZ2 significantly decreased PS exposure and GPIIb/IIIa activation and this inhibition was further pronounced using a combination of both antibodies (Figure 6B-D, Supplementary Figure E-G). OS-1 peptide, an allosteric inhibitor for vWF-GPIbα interaction[68], did not alter the effect of S100A8/A9 on platelets while inhibited vWF-induced platelet agglutination in the presence of ristocetin (Supplementary Figure 4C-D,H-J). The effect of S100A8/A9 was not altered by increasing the concentrations of OS-1 (Supplementary Figure 4H-J). Priming of platelets with S100A8/A9 did not induce platelet agglutination in the presence of vWF (Figure 6E, F). However, S100A8/A9 potentiated vWF-mediated platelet agglutination in the presence of ristocetin (Figure 6E, G). These results show that S100A8/A9 binds to GPIbα, overlapping with vWF-binding sites and potentiates vWF-dependent platelet agglutination.

## GPIbα is the main receptor for S100A8/A9 on human platelets

In order to confirm that GPIbα is the main receptor for S100A8/A9 on human platelets, platelet activation by S100A8/A9 was assessed in the presence of recombinant soluble GPIbα (His-17-Leu505) (rGPIbα), as a competitive inhibition strategy. Human washed platelets failed to respond to S100A8/A9 in the presence of equimolar concentrations of rGPIbα (1.7 μM) (Figure 7A-I). The inhibitory effect was observed for P-selectin

upregulation (Figure 7A-C), PS exposure (Figure 7D-F) and GPIIb/IIIa activation (Figure 7G-H). Furthermore, rGPIbα inhibited the formation of PS positive-MV (Figure 7I).

The key role for GPIb was confirmed using platelets isolated from a patient with Bernard Soulier Syndrome (BSS, deficiency in GPIb-V-IX complex). The patient has a mutation on *GP9* resulting in a defect in GPIb/IX/V complex and the absence of GPIbα expression from platelets (detailed in Supplemental data). Platelets from this patient failed to respond to S100A8/A9, while the response to CRP was normal (Figure 7J-L). S100A8/A9 did not induce P-selectin expression, GPIIb/IIIa activation or PS exposure (Figure 7J-L). These results confirm that GPIbα is the main receptor for S100A8/A9 on human and mouse platelets inducing P-selectin expression, GPIIb/IIIa activation and the formation of procoagulant platelets and platelet-derived PS-positive MVs.

## DISCUSSION

In this study, we identified S100A8/A9-GPIbα interaction as a novel mechanism triggering the formation of procoagulant platelets, independent of platelet aggregation. We show that 1) S100A8/A9 levels are increased in the plasma of patients with COVID-19 and that sustained high levels correlate with adverse outcome; 2) Staining of lung autopsies from fatale COVID-19 cases showed a deposition of S100A8/A9 on lung vessel walls, in neutrophils and a population of CD42b-positive cells; 3) Immobilized recombinant heterodimeric S100A8/A9 accelerated fibrin generation at venous shear; 4) S100A8/A9 heterodimer but not S100A8 or S100A9 monomers/homodimers induced a slow alpha granule secretion, an increase in intracellular $Ca^{2+}$ release and a rapid exposure of PS; 5) S100A8/A9 failed to induce fibrinogen binding and platelet aggregation, despite GPIIb/IIIa activation; 6) S100A8/A9-mediated formation of procoagulant platelet occurred independently of the S100A8/A9 classical receptors RAGE and TLR-4, but it is mediated by the platelet adhesion receptor GPIbα with a supporting role for CD36 and 7) S100A8/A9-mediated platelet activation is resistant to classical anti-platelet drug targeting COX-1 and P2Y12.

Platelet activation and high levels of S100A8/A9 are observed in many thrombo-inflammatory diseases including MI, DVT and infections such as COVID-19[25,33,34,69,70] and these parameters correlate with thrombotic complications. The presence of procoagulant platelets, high cytosolic $Ca^{2+}$ and PS levels were observed in patients with COVID-19 and these levels correlated with increased organ failure assessment score and D-dimer levels and were more pronounced in patients with thrombotic complications[11,71]. Moreover, procoagulant MVs are even detected in non-severe forms of the disease[72,73]. The formation of procoagulant platelets in patients with COVID-19 is partially antibody-driven[71], however alternative pathways might be involved, particularly in the early days following SARS-CoV-2 infection. In accordance to previous reports[25,26,74], we found elevated levels of S100A8/A9 in patients with COVID-19. The levels of S100A8/A9 were higher in severely ill patients and sustained high levels of S100A8/A9 over the first week of monitoring were

observed in non-survivors and associated with worse prognosis. In lung autopsies from fatal COVID-19 cases, S100A8/A9 was found mainly in neutrophils, a population of CD42b-positive cells and on the vessel wall. NETosis, neutrophil necrosis and platelet activation were shown to induce S100A8/A9 release and these levels were further enriched in pathologic conditions[28,75]. Indeed, platelets isolated from COVID-19 patients are enriched in S100A8 and S100A9 mRNA and platelet releasate from COVID-19 patients induces endothelial cell activation *in vitro* in a CD36-dependent manner[28]. In our cohort, S100A9 was detected in platelets while the presence of the S100A8/A9 heterodimer was less pronounced. It was recently shown that neutrophils transfer S100A8 and S100A9 to platelets during NETosis or necrosis and the abundance of S100A8/A9 in platelets depends on neutrophil count in ST-segment–elevation MI (STEMI) patients[69]. Whether platelets contain S100A8 and S100A9 as monomer/homodimers rather than heterodimers with distinct proinflammatory and prothrombotic functions requires further investigation.

As S100A8/A9 deposition on venules support immune cell recruitment and transmigration[29], we assessed its capacity to induce platelet activation and thrombosis at venous shear. While immobilized S100A8/A9 induced platelet adhesion, an increase in intracellular $Ca^{2+}$, the expression of P-selectin and PS-positive platelets and microvesicles, S100A8/A9 alone did not support platelet aggregation and significant fibrin generation at venous shear. However, co-immobilization of S100A8/A9 with collagen accelerated fibrin generation in recalcified blood, which was associated with early recruitment of PS-positive platelets. This procoagulant effect was not observed in PRP, as addition of soluble S100A8/A9 in PRP did not support thrombin generation. This data suggests that immobilized S100A8/A9 rather than plasma soluble S100A8/A9 represents a potent prothrombotic danger signal supporting thrombosis in healthy donors. It is tempting to speculate that S100A8/A9 deposition on the vasculature in COVID-19 patients contributes to the formation of fibrin-rich thrombi.

The early recruitment of PS-positive platelets and subsequent fibrin generation on immobilized S100A8/A9 suggests the formation of procoagulant platelets. The formation of procoagulant platelets *in vitro* is classically studied following co-stimulation of platelets with collagen and thrombin or with $Ca^{2+}$ ionophore A23187, which can lead to the formation of two types of procoagulant platelets, with distinct properties[60]. The first population is associated with a sustained level of intracellular $Ca^{2+}$, depolarized mitochondrial membrane and inactivated GPIIb/IIIa with low capacity to aggregate. The second population retain mitochondrial membrane potential with intracellular $Ca^{2+}$ levels returning to normal, active GPIIb/IIIa and high aggregation properties[60,76–79]. S100A8/A9-induced procoagulant platelets share common features of both populations, which might be due to distinct signaling pathways downstream of S100A8/A9 binding to platelets. S100A8/A9, but not S100A8 or S100A9 alone, induced procoagulant platelets with activated GPIIb/IIIa. However, S100A8/A9-activated platelets failed to bind fibrinogen and to induce platelet aggregation, suggesting the presence of a novel prothrombotic mechanism associated with GPIIb/IIIa activation but independent of platelet aggregation. We further identified GPIbα as the main receptor for S100A8/A9 inducing the formation of procoagulant platelets, both in mice and in human. GPIbα has multiple extracellular agonists including

vWF, thrombin, P-selectin[80] and MAC-1[81] and these interactions regulate thrombosis and inflammation[82]. Using antibodies recognizing epitopes on GPIbα involved in vWF binding, we further show that blocking Leu36-Gln59 region with AK2 antibody[66] or the anionic/sulfated tyrosine region (Tyr276-Glu282) with SZ2 antibody[67] decreased S100A8/A9-induced PS exposure and GPIIb/IIIa activation. These results suggest that S100A8/A9 effect on platelets is regulated by at least two different sites on GPIbα. It is possible that S100A8/A9 binding to these epitopes further affects the engagement of GPIbα with vWF, P-selectin and MAC-1 altering immune cell activation and recruitment, independent of thrombosis. Interestingly, the anionic/sulfated region on GPIbα, with its high negative charge and sulfate groups, shares similarities with heparin, which can bind with high affinity to S100A8/A9[46]. Whether S100A8/A9 binding to this heparin-like sequence on GPIbα induces the formation of procoagulant platelets requires further investigation. S100A8/A9 binding to platelets further potentiates vWF-dependent platelet agglutination in the presence of ristocetin suggesting synergy between S100A8/A9 and vWF. This can be further modulated by CD36 as blockade of the receptor with SSO reduces GPIIb/IIIa activation and PS exposure. Indeed, CD36 was previously shown to partially reduce S100A8/A9-induced thrombosis in mouse models of DVT, photochemical-induced carotid injury and laser-induced injury to the cremaster microcirculation[27,34]. Our data support the contribution of CD36 to platelet GPIIb/IIIa activation and PS exposure without affecting P-selectin expression. It is likely that the initial interaction occurs through GPIbα with crosstalk between GPIbα and CD36, essential for platelet activation[83].

In conclusion, our study identified for the first time the S100A8/A9-GPIbα interaction as a novel driver for the formation of procoagulant platelets accelerating fibrin generation. Despite GPIIb/IIIa activation, platelets failed to bind to fibrinogen suggesting that this mechanism of thrombosis is independent of platelet aggregation. Importantly, existing drugs can block distinct pathways, with Syk inhibitors reducing P-selectin expression on platelets and subsequent platelet-neutrophil aggregates. However, inhibition of GPIbα alone or in conjunction with CD36 is essential to limit PS exposure and GPIIb/IIIa activation. As this novel mechanism is resistant to classical or emerging anti-platelet or anti-S100A8/A9 drugs, this study supports the need for the development of novel therapies to limit the formation of procoagulant platelets in thrombo-inflammatory diseases associated with the release of S100A8/A9 such as COVID-19.



**Acknowledgements:** JR holds a British Heart Foundation (BHF) Intermediate Fellowship (FS/IBSRF/20/25039). This research was partially supported by a BHF project grant (PG/21/10737), the BHF Accelerator Award (AA/18/2/34218), UK Spine Knowledge exchange (R78606/CN003) and the Medical Research Council [grant number MC_PC_19029] for JR. MC is supported by Wellcome Trust 4 Year PhD studentship program on Mechanisms of Inflammatory Disease (204951). AA are supported by the Austrian Science Fund (P32064 and P34783). GP is supported by a Birmingham-Maastricht studentship. SPW holds a BHF Chair (CH03/003). AOK is a Henry Wellcome

fellow (218649/Z/19/Z). NJM is supported by University of Aberdeen Development Trust and NHS Grampian Endowment funds (COV19-004 and 20/021). AJI holds a Birmingham fellowship. We thank Beata Grygielska for genotyping mice and University of Birmingham Enterprise Ltd or the translational Research Team for their support. A CC BY or equivalent licence is applied to AAM arising from this submission, in accordance with the grant's open access conditions.

## Author contributions

MC designed and performed experiments, collected and analyzed data and wrote the manuscript; WCS, GP, MJS, JP, JCC, JB, JSR, ZZ, AS performed experiments and analyzed data; JHB and AOK analyzed data; MP, NSP; PLRN, PH, AJI, GER, SPW and MRT provided key reagents and contributed to data analysis; NJM and AA provided key reagents and supported research design and analysis; JR designed research and experiments, performed experiments, collected and analyzed data and wrote the manuscript. All authors read and approved the paper.

**Conflict of interest:** This work is protected by UoB patent (patent application number: PCT/GB2022/052007).

**Legends:**

**Figure 1: S100A8/A9 accelerates the recruitment of Annexin-V-positive platelets and fibrin generation at a venous shear rate.** (**A**, **B**, **C**) Plasma levels of S100A8/A9 were measured by ELISA in healthy donors and patients with uncomplicated and complicated (ICU survivors/non-survivors) COVID-19 over seven consecutive days following inclusion in the study. (**A**) S100A8/A9 levels in the plasma of healthy donors (control, n=10), uncomplicated COVID-19 patients (n=48), ICU-survivors (n=26) and ICU non-survivors (n=13) on the first day of patient inclusion in the study. (**B**, **C**) S100A8/A9 level in the plasma over 7 consecutive days following patient recruitment. **(D, E, F, G)** Representative Immunofluorescence staining of lung autopsies obtained from COVID-19 patients or age-matched control. Images were captured using Epi fluorescence microscope and slide scanner Axioscan Z1. **(D)** Platelet CD42b and heterodimeric S100A8/A9 staining in lung parenchyma and microcirculation in COVID-19 and control lung autopsies. **(E)** Staining for S100A8/A9, MPO, and nuclei (DAPI) of a large vessel in the lung of a patient with COVID-19 with thrombotic complications. **(F)** Staining for platelet CD42b, fibrin, and nuclei (DAPI) in large thrombi of a patient with COVID-19. (**G**) S100A9, CD42 and fibrin staining in COVID-19 lung. Arrow shows platelet-fibrin microaggregates. (**H**) Whole blood under recalcified conditions was perfused at a venous shear rate (100 $s^{-1}$) over S100A8/A9 (40 µg/ml), collagen (100 µg/ml) or combination of S100A8/A9 and collagen-coated chambers. The presence PS-positive platelets and fibrin were assessed using Annexin-V-AlexaFluor-647 and FITC-anti-fibrinogen/fibrin antibody, respectively. (**H**) Representative images taken at 15 minutes. **(I)** Quantification of Annexin-V signal (3 min) (n=5) and (**J**) fibrin signal time course (0-15min) (n=5) using pre-defined semi-automated scripts in Fiji as detailed in supplemental methods. Results are shown as mean ± SEM. The statistical significance was analyzed using two-way ANOVA with Tukey's multiple comparison Test between all groups. ∗ p<0.05, ∗∗ p<0.005, ∗∗∗p<0.001, ∗∗∗∗ p<0.0001.

**Figure 2. Recombinant S100A8/A9 induces human platelet activation *in vitro*.** Human washed platelets ($10^6$ platelets/condition) were incubated with different concentrations of recombinant heterodimeric S100A8/A9 (10, 20 and 40 µg/ml) for 30 min at 37 °C. (**A**, **B**) Platelet activation was determined by flow cytometry using anti-P-selectin antibody. **(A)** Representative plots from a healthy donor, histograms normalized to mode (each peak normalized to its mode for each condition). **(B)** Percentage of $CD41^+$P-$selectin^+$ platelets. **(C)** The percentage of platelet-neutrophil aggregates ($CD66b^+/CD41^+$) in whole blood following addition of S100A8/A9 for 30 min at 37 °C (n=7). Blood was diluted 1:5. **(D)** Anti-CD41/CD61 PAC-1 antibody (against activated GPIIb/IIIa) binding to platelets was assessed by flow cytometry and presented as percentage of $CD41^+$ platelets-positive for PAC-1 (n=17). **(E, F)** Washed platelets ($2x10^8$/ml) were incubated with S100A8/A9 (40 µg/ml) or CRP (10 µg/ml) and platelet aggregation assessed for 20 min by light transmission aggregometry (n=3). (**G, H**) Washed platelets ($2x10^8$/ml) were incubated

with S100A8/A9 (40 µg/ml) or CRP (10 µg/ml) and ATP generation assessed for 6 min the CHRONO-LUME® luciferin:luciferase assay kit from Chronolog (n=3). (**E, G**) representative traces. (**I**, **J**) Washed platelets ($2x10^8$/ml) were incubated with S100A8/A9 (20 µg/ml or 40 µg/ml) for 6 minutes under stirring condition followed by depleted fibrinogen (200 µg/ml) and platelet aggregation assessed for 6 min by light transmission aggregometry (n=3). **(K, L)** Alexa-fluor 488-labelled fibrinogen binding to platelets. **(K)** Representative plot for fibrinogen binding. **(L)** Percentage of platelets-positive for fibrinogen-Alexa 488. CRP (10 µg/ml) and TRAP-6 (100 µM) were used as positive control. Data is shown as mean ± SD. The statistical significance was analyzed using ordinary one-way ANOVA. ∗ p<0.05, ∗∗ p<0.005, ∗∗∗p<0.001, ∗∗∗∗ p<0.0001.

**Figure 3. S100A8/A9 induces the formation of procoagulant platelets.** Human washed platelets ($10^6$ platelets/condition) were incubated with different concentrations of S100A8/A9 (10, 20 and 40 µg/ml) for 30 min at 37°C. (**A**, **B**, **C**) Phosphatidylserine exposure was determined by flow cytometry using PE-Cy7-labelled Annexin-V (n=17). CRP (10 µg/ml) and TRAP-6 (100 µM) were used as positive control. (**A**) Representative histogram for Annexin-V staining. Representative histograms normalized to mode (each peak normalized to its mode for each condition). **(B)** Percentage of $CD41^+Annexin\text{-}V^+$ platelets. (**C**) Fold change in the MFI (Mean Fluorescent Intensity) of agonist-activated platelets over control. **(D)** The percentage of $CD41^+$ microvesicles (MV) positive for Annexin-V (n=6). **(E, F)** Human washed platelets spreading on collagen or S100A8/A9. I Representative differential interference contrast (DIC) images of spread platelets. (**F**) Representative Annexin-V (magenta) and P-selectin (green) staining for adherent platelets. **(G)** Quantification of Annexin-V-positive or P-selectin-positive or Annexin-V and P-selectin-double positive platelets of platelet adhesion on collagen and S100A8/A9 (Positive platelets/total platelets). The statistical significance was analyzed using two-way ANOVA with Tukey's multiple comparison Test between all groups. (**H**, **I**) Assessment of intracellular $Ca^{2+}$ release from platelets spread over surfaces coated with either S100A8/A9 (20 and 40 µg/ml), fibrinogen or BSA assessed using BAPTA-1-AM calcium sensitive dye. (**H**) Representative $Ca^{2+}$ traces assessed using oregon green-488 BAPTA-1-AM. (**I**) Peak fluorescence at time point zero (F0/Fmax). Data is shown as mean ± SD. The statistical significance was analyzed using nonparametric test (Kruskal-Wallis Test). ∗ p<0.05, ∗∗ p<0.005, ∗∗∗p<0.001, ∗∗∗∗ p<0.0001.

**Figure 4. CD36 blockade partially decreases GPIIb/IIIa activation and phosphatidylserine exposure whereas ITAM receptor inhibition reduces P-selectin expression.** Human washed platelets ($10^6$ platelets/condition) were incubated with S100A8/A9 (20 µg/ml) with or without different inhibitors for 30 min at 37 °C. Inhibitors were preincubated with platelets for 10 min prior to addition of S100A8/A9: Paquinimod (blocks S100A8/A9 binding to RAGE and TLR4) (10 µM), RAGE inhibitor Azeliragon (1

μM), CD36 inhibitor Sulfosuccinimidyl oleate (SSO, 25 μM), Syk inhibitor PRT-060318 (10 μM) Src inhibitor PP2 (20 μM), BTK inhibitor Ibrutinib (500 nM) were used. Platelet activation was determined by flow cytometry using (**A, D, G**) anti-CD41/CD61 PAC-1 antibody, (**B, E, H**) anti-P-selectin antibody and (**C**, **F**, **I**) Annexin-V binding. Data is shown as the percentage of platelets positive ($CD41^+$) for these markers. Data is shown as mean ± SD. Statistical significance was analyzed using ordinary one-way ANOVA. ✱ p<0.05, ✱✱ p<0.005, ✱✱✱ p<0.001, ✱✱✱✱ p<0.0001.

**Figure 5. Murine S100A8/A9 activates mouse platelets through GPIbα and CD36.** Washed murine platelets ($10^6$ platelets/condition) were incubated with different doses of S100A8/A9 for 30 min at 37 °C (**A**). Platelet activation was determined by flow cytometry using anti-P-selectin antibody and (**B**) Annexin-V binding. (**C-K**,). Washed platelets isolated from wild type (WT), GPVI ($GPVI^{-/-}$), CLEC-2 ($CLEC\text{-}2^{-/-}$), GPVI/CLEC-2 knock-out ($GPVI^{-/-}$/$CLEC\text{-}2^{-/-}$) or $GPIb\alpha^{-/-}$ mice (IL4R/GPIbα−Tg mice) were incubated with S100A8/A9 (10 μg/ml) for 30 min at 37°C. The percentage of platelets positive for P-selectin, GPIIb/IIIa activation (JON/A) and Annexin-V binding were measured by flow cytometry. Data is shown as percentage platelets ($CD41^+$) positive for different markers. (**K**) Platelets isolated from WT or IL4R/GPIbα−Tg mice were pretreated with SSO (25 μg/ml) prior to addition of S100A8/A9 (10 μg/ml) for 30 min at 37 °C and Annexin-V binding assessed by flow cytometry. The statistical significance was analyzed using nonparametric test (Kruskal-WallisTest) for A, B, ordinary 2-way ANOVA with Sidak's multiple comparison test for C, D, F, H, J and 2-way ANOVA with Tukey's multiple comparison test for 5K. Data is shown as mean ± SD. ✱ p<0.05, ✱✱ p<0.005, ✱✱✱ p<0.001.

**Figure 6. GPIbα binds to S100A8/A9 independently of vWF binding site. (A)** The dose-binding curves of rGPIbα on S100A8/A9-coated surfaces (S100A8/A9 0.5 μg/ml). Data presented as mean ± SEM (n=3). **(B, C, D)** Washed human platelets ($10^6$/condition) were pre-incubated with or without AK2 Ab (40 μg/ml), SZ2 (40 μg/ml), or both for 10 min at 37 °C and then stimulated with S100A8/A9 (20 μg/ml) for other 30 minutes at 37 °C. Platelet activation was determined by flow cytometry using **(B)** Anti-CD41/CD61 PAC-1 antibody, (**C**) anti-P-selectin antibody and (**D**) Annexin-V binding. Data is shown as percentage platelets ($CD41^+$) positive for different markers. **(E, F, G)** Ristocetin-induced platelet aggregation was assessed by addition of vWF (1 μg/ml) and ristocetin (1.5 mg/ml) to washed platelets. Platelets were primed with S100A8/A9 and ristocetin for 6 min before addition of vWF. Platelet aggregation was monitored for 6 min following vWF addition (n=6). (**E**) Representative trace. Data is shown as mean ± SEM. The statistical significance was analyzed using ordinary one-way ANOVA (B, C, D) and non-parametric

Mann-Whitney T-test (Kruskal-Wallis Test) (F, G). ∗ p<0.05, ∗∗ p<0.01, ∗∗∗ p<0.001, ∗∗∗∗ p<0.0001.

**Figure 7. Recombinant human GPIbα blocks platelet response to S100A8/A9 while Bernard-Soulier Syndrome (BSS) platelets failed to respond to S100A8/A9.** Washed human platelets ($10^6$ platelets/condition) were incubated with S100A8/A9 (40 µg/ml; 1.7 µM) in the absence or presence of recombinant human GPIbα (rGPIbα; 1.7 µM) for 30 min at 37 °C (n=3). Platelet activation was assessed by flow cytometry using **(A, B, C)** anti-P-selectin, (**D, E, F**) PS exposure using Annexin-V and **(G, H, I)** GPIIb/IIIa activation using PAC-1 antibody**.** Human washed platelets from a healthy donor or BSS patient were incubated with S100A8/A9 (20 and 40 µg/ml) for 30 min at 37 $^{o}$C (**J, K, L**). CRP (10 µg/ml) was used as positive control. (**J**) GPIIb/IIIa activation, (**K**) P-selectin and (**L**) PS exposure were measured. The statistical significance was analyzed using one-way ANOVA. Data presented as mean ± SEM. ∗ p<0.05, ∗∗ p<0.005, ∗∗∗ p<0.001, ∗∗∗∗ p<0.0001.

## References


1. Russwurm S, Vickers J, Meier-Hellmann A, et al. Platelet and leukocyte activation correlate with the severity of septic organ dysfunction. *Shock*. 2002;17(4):263–268.
2. Nicolai L, Massberg S. Platelets as key players in inflammation and infection. *Curr. Opin. Hematol.* 2020;27(1):34–40.
3. Lievens D, Zernecke A, Seijkens T, et al. Platelet CD40L mediates thrombotic and inflammatory processes in atherosclerosis. *Blood*. 2010;116(20):4317–4327.
4. Zhou J, Xu E, Shao K, et al. Circulating platelet-neutrophil aggregates as risk factor for deep venous thrombosis. *Clin. Chem. Lab. Med.* 2019;57(5):707–715.
5. Marquardt L, Anders C, Buggle F, et al. Leukocyte-Platelet Aggregates in Acute and Subacute Ischemic Stroke. *Cerebrovasc. Dis.* 2009;28(3):276–282.
6. Ren F, Mu N, Zhang X, et al. Increased Platelet-leukocyte Aggregates Are Associated With Myocardial No-reflow in Patients With ST Elevation Myocardial Infarction. *Am. J. Med. Sci.* 2016;352(3):261–266.
7. Schrottmaier WC, Mussbacher M, Salzmann M, Assinger A. Platelet-leukocyte interplay during vascular disease. *Atherosclerosis*. 2020;307:109–120.
8. GAWAZ M, FATEH-MOGHADAM S, PILZ G, GURLAND H -J, WERDAN K. Platelet

activation and interaction with leucocytes in patients with sepsis or multiple organ failure. *Eur. J. Clin. Invest.* 1995;25(11):843–851.

9. Koupenova M, Corkrey HA, Vitseva O, et al. The role of platelets in mediating a response to human influenza infection. *Nat. Commun. 2019 101*. 2019;10(1):1–18.

10. Hottz ED, Azevedo-Quintanilha IG, Palhinha L, et al. Platelet activation and platelet-monocyte aggregate formation trigger tissue factor expression in patients with severe COVID-19. 2020;

11. Khattab MH, Prodan CI, Vincent AS, et al. Increased procoagulant platelet levels are predictive of death in COVID-19. *GeroScience*. 2021;43(4):2055.

12. Yatim N, Boussier J, Chocron R, et al. Platelet activation in critically ill COVID-19 patients. *Ann. Intensive Care 2021 111*. 2021;11(1):1–12.

13. Rondina MT, Carlisle M, Fraughton T, et al. Platelet–Monocyte Aggregate Formation and Mortality Risk in Older Patients With Severe Sepsis and Septic Shock. *Journals Gerontol. Ser. A*. 2015;70(2):225–231.

14. P V, S G, PC A, et al. Histone H4 induces platelet ballooning and microparticle release during trauma hemorrhage. *Proc. Natl. Acad. Sci. U. S. A.* 2019;116(35):17444–17449.

15. Khismatullin RR, Ponomareva AA, Nagaswami C, et al. Pathology of lung-specific thrombosis and inflammation in COVID-19. *J. Thromb. Haemost.* 2021;00:1–11.

16. Loeffen R, Godschalk TC, Oerle R van, et al. The hypercoagulable profile of patients with stent thrombosis. *Heart*. 2015;101(14):1126–1132.

17. Morel O, Jesel L, Freyssinet J, Toti F. Elevated levels of procoagulant microparticles in a patient with myocardial infarction, antiphospholipid antibodies and multifocal cardiac thrombosis. *Thromb. J. 2005 31*. 2005;3(1):1–5.

18. Shannon O. The role of platelets in sepsis. *Res. Pract. Thromb. Haemost.* 2021;5(1):27–37.

19. Kerris EWJ, Hoptay C, Calderon T, Freishtat RJ. Platelets and platelet extracellular vesicles in hemostasis and sepsis. *J. Investig. Med.* 2020;68(4):813–820.

20. M L, M R, B L, et al. Enhanced platelet-derived microparticle formation is associated with carotid atherosclerosis in convalescent stroke patients. *Platelets*. 2013;24(1):63–70.

21. CI P, JA S, LD C, GL D. Higher coated-platelet levels are associated with stroke recurrence following nonlacunar brain infarction. *J. Cereb. Blood Flow Metab.* 2013;33(2):287–292.

22. CI P, AS V, GL D. Coated-platelet levels are elevated in patients with transient ischemic attack. *Transl. Res.* 2011;158(1):71–75.

23. Gould TJ, Lysov Z, Liaw PC. Extracellular DNA and histones: double-edged swords in immunothrombosis. *J. Thromb. Haemost.* 2015;13(S1):S82–S91.

24. S K, A O, L N. The role of neutrophils in thrombosis. *Thromb. Res.* 2018;170:87–96.

25. Q G, Y Z, J L, et al. Induction of alarmin S100A8/A9 mediates activation of aberrant neutrophils in the pathogenesis of COVID-19. *Cell Host Microbe*. 2021;29(2):222-235.e4.

26. Mahler M, Meroni P-LL, Infantino M, Buhler KA, Fritzler MJ. Circulating Calprotectin as a Biomarker of COVID-19 Severity. *https://doi.org/10.1080/1744666X.2021.1905526*. 2021;17(5):431–443.

27. Wang Y, Fang C, Gao H, et al. Platelet-derived S100 family member myeloid-related protein-14 regulates thrombosis. *J. Clin. Invest.* 2014;124(5):2160–2171.

28. Barrett TJ, Cornwell M, Myndzar K, et al. Platelets amplify endotheliopathy in COVID-19. *Sci. Adv.* 2021;7(37):.

29. Hogg N, Allen C, Edgeworth J. Monoclonal antibody 5.5 reacts with p8,14, a myeloid molecule associated with some vascular endothelium. *Eur. J. Immunol.* 1989;19(6):1053–1061.

30. Frangogiannis NG. S100A8/A9 as a therapeutic target in myocardial infarction: cellular mechanisms, molecular interactions, and translational challenges. *Eur. Heart J.* 2019;40(32):2724–2726.

31. Schiopu A, Marinkovic G, DeCamp L, et al. The S100A8/A9 alarmin stimulates myeloid cell response and promotes cardiac repair after myocardial infarction. *Atherosclerosis*. 2018;275:e7.

32. Schiopu A, Cotoi OS. S100A8 and S100A9: DAMPs at the crossroads between innate immunity, traditional risk factors, and cardiovascular disease. *Mediators Inflamm.* 2013;2013:.

33. Dubois C, Marcé D, Faivre V, et al. High plasma level of S100A8/S100A9 and S100A12 at admission indicates a higher risk of death in septic shock patients. *Sci. Reports 2019 91*. 2019;9(1):1–7.

34. Wang Y, Gao H, Kessinger CW, et al. Myeloid-related protein-14 regulates deep vein thrombosis. 2017;2(11):.

35. Geven EJW, van den Bosch MHJ, Di Ceglie I, et al. S100A8/A9, a potent serum and molecular imaging biomarker for synovial inflammation and joint destruction in seronegative experimental arthritis. *Arthritis Res. Ther.* 2016;18(1):1–12.

36. Okada K, Okabe M, Kimura Y, Itoh H, Ikemoto M. Serum S100A8/A9 as a Potentially Sensitive Biomarker for Inflammatory Bowel Disease. *Lab. Med.* 2019;50(4):370–380.

37. Müller I, Vogl T, Kühl U, et al. Serum alarmin S100A8/S100A9 levels and its potential role as biomarker in myocarditis. *ESC Hear. Fail.* 2020;7(4):1442–1451.

38. Wang S, Song R, Wang Z, et al. S100A8/A9 in Inflammation. *Front. Immunol.* 2018;0(JUN):1298.

39. Zhong X, Xie F, Chen L, Liu Z, Wang Q. S100A8 and S100A9 promote endothelial cell activation through the RAGE-mediated mammalian target of rapamycin complex 2 pathway. *Mol. Med. Rep.* 2020;22(6):5293–5303.

40. Edgeworth J, Gormanl M, Bennett R, Freemontl P, Hogg N. THE JOURNAL OF BIOLOGICAL CHEMISTRY Identification of p8,14 as a Highly Abundant Heterodimeric Calcium Binding Protein Complex of Myeloid Cells*. *J. Biol. Chem.* 1991;266(12):7706–7713.

41. Hessian PA, Edgeworth J, Hogg N. MRP-8 and MRP-14, two abundant Ca2+-binding proteins of neutrophils and monocytes. *J. Leukoc. Biol.* 1993;53(2):197–204.

42. Chen B, Miller AL, Rebelatto M, et al. S100A9 Induced Inflammatory Responses Are Mediated by Distinct Damage Associated Molecular Patterns (DAMP) Receptors In Vitro and In Vivo. *PLoS One*. 2015;10(2):e0115828.

43. Fuentes E, Rojas A, Palomo I. Role of multiligand/RAGE axis in platelet activation. *Thromb. Res.* 2014;133(3):308–314.

44. A G, G M, K C, et al. Platelet CD36 surface expression levels affect functional responses

to oxidized LDL and are associated with inheritance of specific genetic polymorphisms. *Blood*. 2011;117(23):6355–6366.

45. Assinger A, Schrottmaier WC, Salzmann M, Rayes J. Platelets in Sepsis: An Update on Experimental Models and Clinical Data. *Front. Immunol.* 2019;0(JULY):1687.

46. Robinson MJ, Tessier P, Poulsom R, Hogg N. The S100 Family Heterodimer, MRP-8/14, Binds with High Affinity to Heparin and Heparan Sulfate Glycosaminoglycans on Endothelial Cells *. *J. Biol. Chem.* 2002;277(5):3658–3665.

47. Kerkhoff C, Sorg C, Tandon NN, Nacken W. Interaction of S100A8/S100A9-arachidonic acid complexes with the scavenger receptor CD36 may facilitate fatty acid uptake by endothelial cells. *Biochemistry*. 2001;40(1):241–248.

48. Mussbacher M, Schrottmaier WC, Salzmann M, et al. Optimized plasma preparation is essential to monitor platelet-stored molecules in humans. 2017;12(12):e0188921.

49. Khan AO, Reyat JS, Bourne JH, et al. Stimulation of vascular organoids with SARS-CoV-2 antigens increases endothelial permeability and regulates vasculopathy. *medRxiv*. 2021;2021.04.25.21255890.

50. Futami J, Atago Y, Azuma A, et al. An efficient method for the preparation of preferentially heterodimerized recombinant S100A8/A9 coexpressed in Escherichia coli. *Biochem. Biophys. Reports*. 2016;6:94.

51. Hughes CE, Pollitt AY, Mori J, et al. CLEC-2 activates Syk through dimerization. *Blood*. 2010;115(14):2947–2955.

52. Nicolson PLR, Hughes CE, Watson S, et al. Inhibition of Btk by Btk-specific concentrations of ibrutinib and acalabrutinib delays but does not block platelet aggregation mediated by glycoprotein VI. *Haematologica*. 2018;103(12):2097–2108.

53. Zuo Y, Zuo M, Yalavarthi S, et al. Neutrophil extracellular traps and thrombosis in COVID-19. *J. Thromb. Thrombolysis 2020 512*. 2020;51(2):446–453.

54. Silvin A, Chapuis N, Dunsmore G, et al. Elevated Calprotectin and Abnormal Myeloid Cell Subsets Discriminate Severe from Mild COVID-19. 2020;

55. Schrottmaier WC, Pirabe A, Pereyra D, et al. Platelets and Antiplatelet Medication in COVID-19-Related Thrombotic Complications. *Front. Cardiovasc. Med.* 2022;8:.

56. Schrottmaier WC, Pirabe A, Pereyra D, et al. Adverse Outcome in COVID-19 Is Associated With an Aggravating Hypo-Responsive Platelet Phenotype. *Front. Cardiovasc. Med.* 2021;8:.

57. Schenten V, Plançon S, Jung N, et al. Secretion of the phosphorylated form of S100A9 from neutrophils is essential for the proinflammatory functions of extracellular S100A8/A9. *Front. Immunol.* 2018;9(MAR):

58. Shrivastava S, Chelluboina S, Jedge P, et al. Elevated Levels of Neutrophil Activated Proteins, Alpha-Defensins (DEFA1), Calprotectin (S100A8/A9) and Myeloperoxidase (MPO) Are Associated With Disease Severity in COVID-19 Patients. *Front. Cell. Infect. Microbiol.* 2021;11:.

59. Chen L, Long X, Xu Q, et al. Elevated serum levels of S100A8/A9 and HMGB1 at hospital admission are correlated with inferior clinical outcomes in COVID-19 patients. *Cell. Mol. Immunol. 2020 179*. 2020;17(9):992–994.

60. Topalov NN, Yakimenko AO, Canault M, et al. Two Types of Procoagulant Platelets Are Formed Upon Physiological Activation and Are Controlled by Integrin αIIbβ3. *Arterioscler. Thromb. Vasc. Biol.* 2012;32(10):2475–2483.

61. Yang M, Cooley BC, Li W, et al. Platelet CD36 promotes thrombosis by activating redox sensor ERK5 in hyperlipidemic conditions. *Blood*. 2017;129(21):2917–2927.

62. Ding N, Chen G, Hoffman R, et al. TLR4 Regulates Platelet Function and Contributes to Coagulation Abnormality and Organ Injury in Hemorrhagic Shock and Resuscitation. *Circ. Cardiovasc. Genet.* 2014;7(5):615.

63. I A, YC C, D T, et al. HMGB1 binds to activated platelets via the receptor for advanced glycation end products and is present in platelet rich human coronary artery thrombi. *Thromb. Haemost.* 2015;114(5):994–1003.

64. Ozaki Y, Suzuki-Inoue K, Inoue O. Platelet receptors activated via mulitmerization: glycoprotein VI, GPIb-IX-V, and CLEC-2. *J. Thromb. Haemost.* 2013;11 Suppl 1(SUPPL.1):330–339.

65. Heit B, Kim H, Cosío G, et al. Multimolecular signaling complexes enable Syk-mediated signaling of CD36 internalization. *Dev. Cell*. 2013;24(4):372–383.

66. Shen Y, Romo GM, Dong JF, et al. Requirement of leucine-rich repeats of glycoprotein

(GP) Ibα for shear-dependent and static binding of von Willebrand factor to the platelet membrane GP Ib–IX-V complex. *Blood*. 2000;95(3):903–910.

67. Ward CM, Andrews RK, Smith AI, Berndt MC. Mocarhagin, a Novel Cobra Venom Metalloproteinase, Cleaves the Platelet von Willebrand Factor Receptor Glycoprotein Ibα. Identification of the Sulfated Tyrosine/Anionic Sequence Tyr-276−Glu-282 of Glycoprotein Ibα as a Binding Site for von Willebrand Fact. *Biochemistry*. 1996;35(15):4929–4938.

68. McEwan PA, Andrews RK, Emsley J. Glycoprotein Ibα inhibitor complex structure reveals a combined steric and allosteric mechanism of von Willebrand factor antagonism. *Blood*. 2009;114(23):4883–4885.

69. Joshi A, Schmidt LE, Burnap SA, et al. Neutrophil-Derived Protein S100A8/A9 Alters the Platelet Proteome in Acute Myocardial Infarction and Is Associated with Changes in Platelet Reactivity. *Arterioscler. Thromb. Vasc. Biol.* 2022;42(1):49–62.

70. Mellett L, Khader SA. S100A8/A9 in COVID-19 pathogenesis: Impact on clinical outcomes. *Cytokine Growth Factor Rev.* 2022;63:90–97.

71. Althaus K, Marini I, Zlamal J, et al. Antibody-induced procoagulant platelets in severe COVID-19 infection. *Blood*. 2021;137(8):1061–1071.

72. Wool GD, Miller JL. The Impact of COVID-19 Disease on Platelets and Coagulation. *Pathobiology*. 2021;88(1):15–27.

73. Puhm F, Allaeys I, Lacasse E, et al. Platelet activation by SARS-CoV-2 implicates the release of active tissue factor by infected cells. *Blood Adv.* 2022;

74. Canzano P, Brambilla M, Porro B, et al. Platelet and Endothelial Activation as Potential Mechanisms Behind the Thrombotic Complications of COVID-19 Patients. *JACC Basic to Transl. Sci.* 2021;6(3):202–218.

75. Sprenkeler EGG, Zandstra J, van Kleef ND, et al. S100A8/A9 Is a Marker for the Release of Neutrophil Extracellular Traps and Induces Neutrophil Activation. *Cells 2022, Vol. 11, Page 236*. 2022;11(2):236.

76. R van K, NJ M, C S, et al. Both TMEM16F-dependent and TMEM16F-independent pathways contribute to phosphatidylserine exposure in platelet apoptosis and platelet activation. *Blood*. 2013;121(10):1850–1857.

77. HJ C, TB S, L M, MB W, SM J. Mitochondrial calcium and reactive oxygen species regulate agonist-initiated platelet phosphatidylserine exposure. *Arterioscler. Thromb. Vasc. Biol.* 2012;32(12):2946–2955.

78. Dale GL. Procoagulant Platelets: Further Details but Many More Questions. *Arterioscler. Thromb. Vasc. Biol.* 2017;37(9):1596–1597.

79. Agbani EO, Poole AW. Procoagulant platelets: generation, function, and therapeutic targeting in thrombosis. *Blood*. 2017;130(20):2171–2179.

80. Peyvandi F, Garagiola I, Baronciani L. Role of von Willebrand factor in the haemostasis. *Blood Transfus.* 2011;9(Suppl 2):s3.

81. Wang Y, Gao H, Shi C, et al. Leukocyte integrin Mac-1 regulates thrombosis via interaction with platelet GPIbα. *Nat. Commun. 2017 81*. 2017;8(1):1–16.

82. Denorme F, Vanhoorelbeke K, De Meyer SF. von Willebrand Factor and Platelet Glycoprotein Ib: A Thromboinflammatory Axis in Stroke. *Front. Immunol.* 2019;10:2884.

83. Döhrmann M, Makhoul S, Gross K, et al. CD36-fibrin interaction propagates FXI-dependent thrombin generation of human platelets. *FASEB J.* 2020;34(7):9337–9357.

Figure 1

A

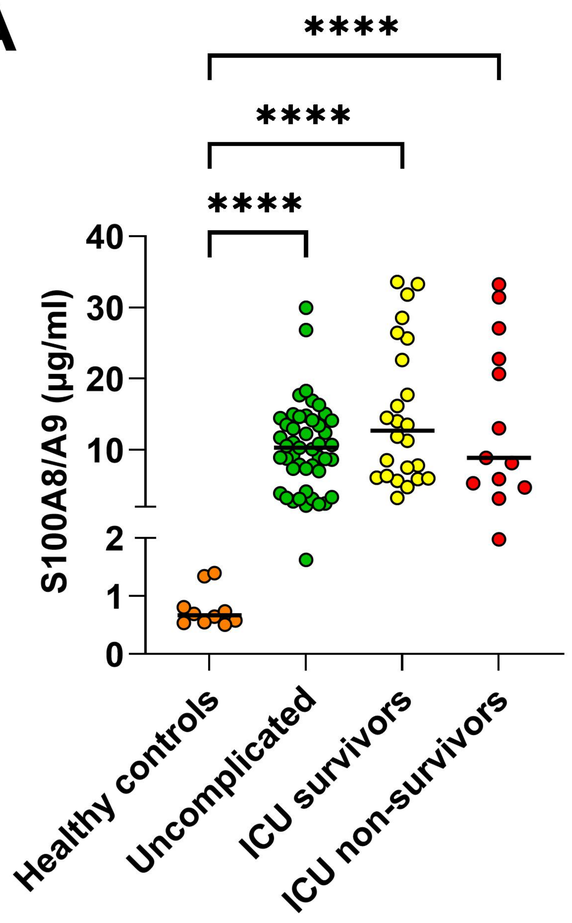


B

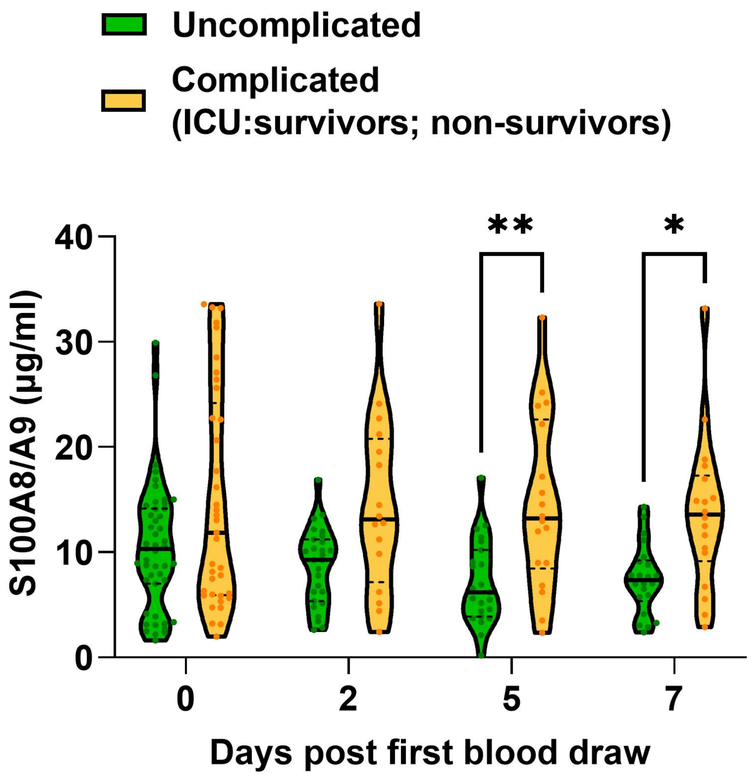


C

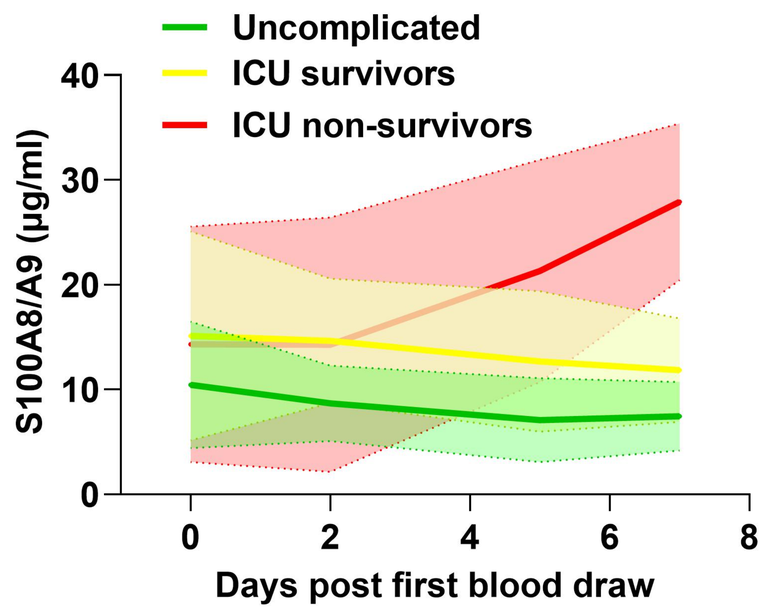


D

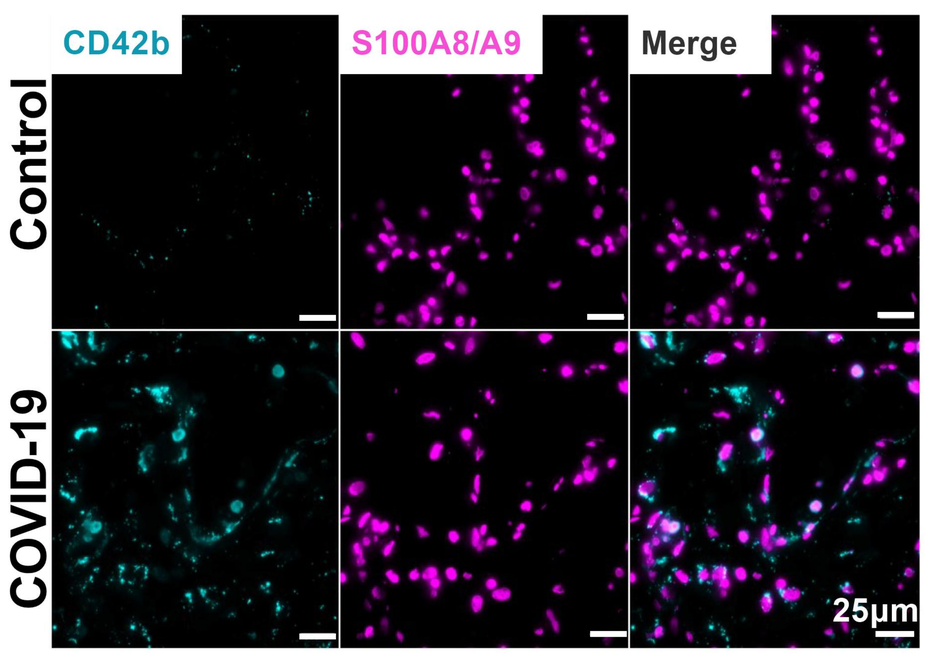


E

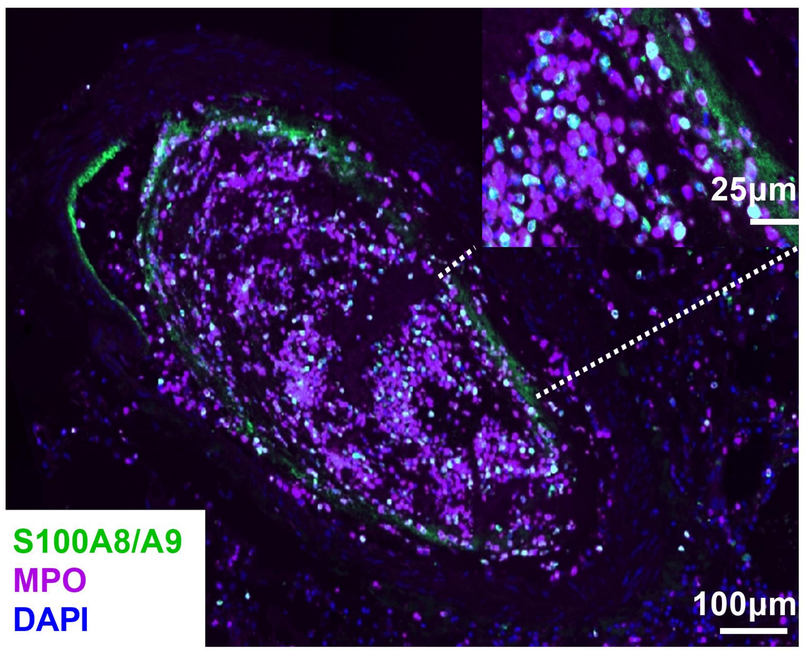


F

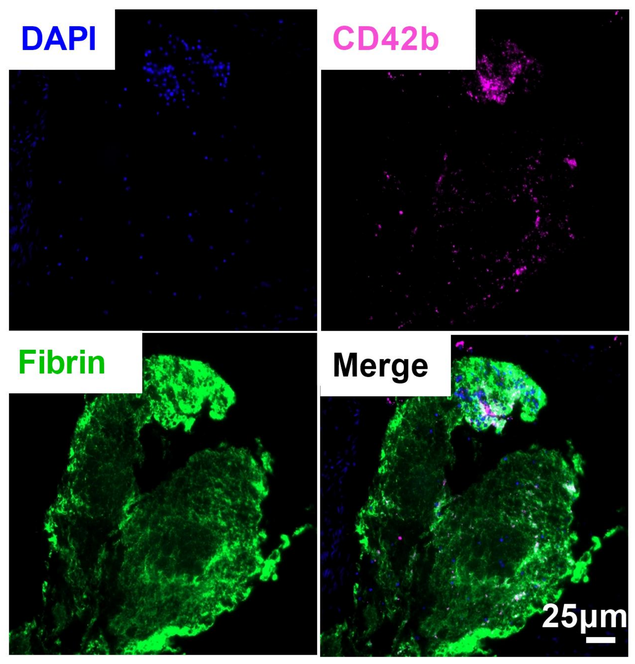


G

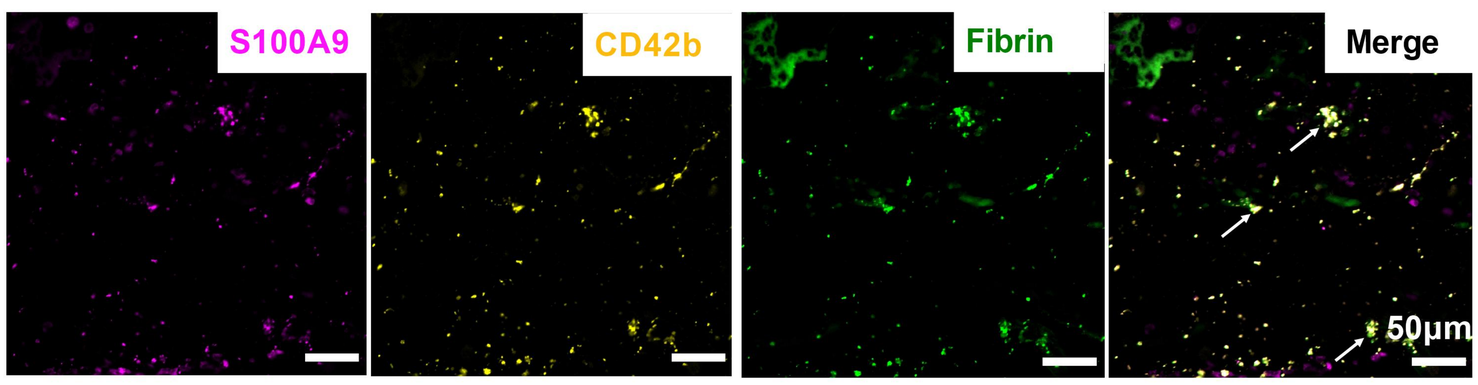


H

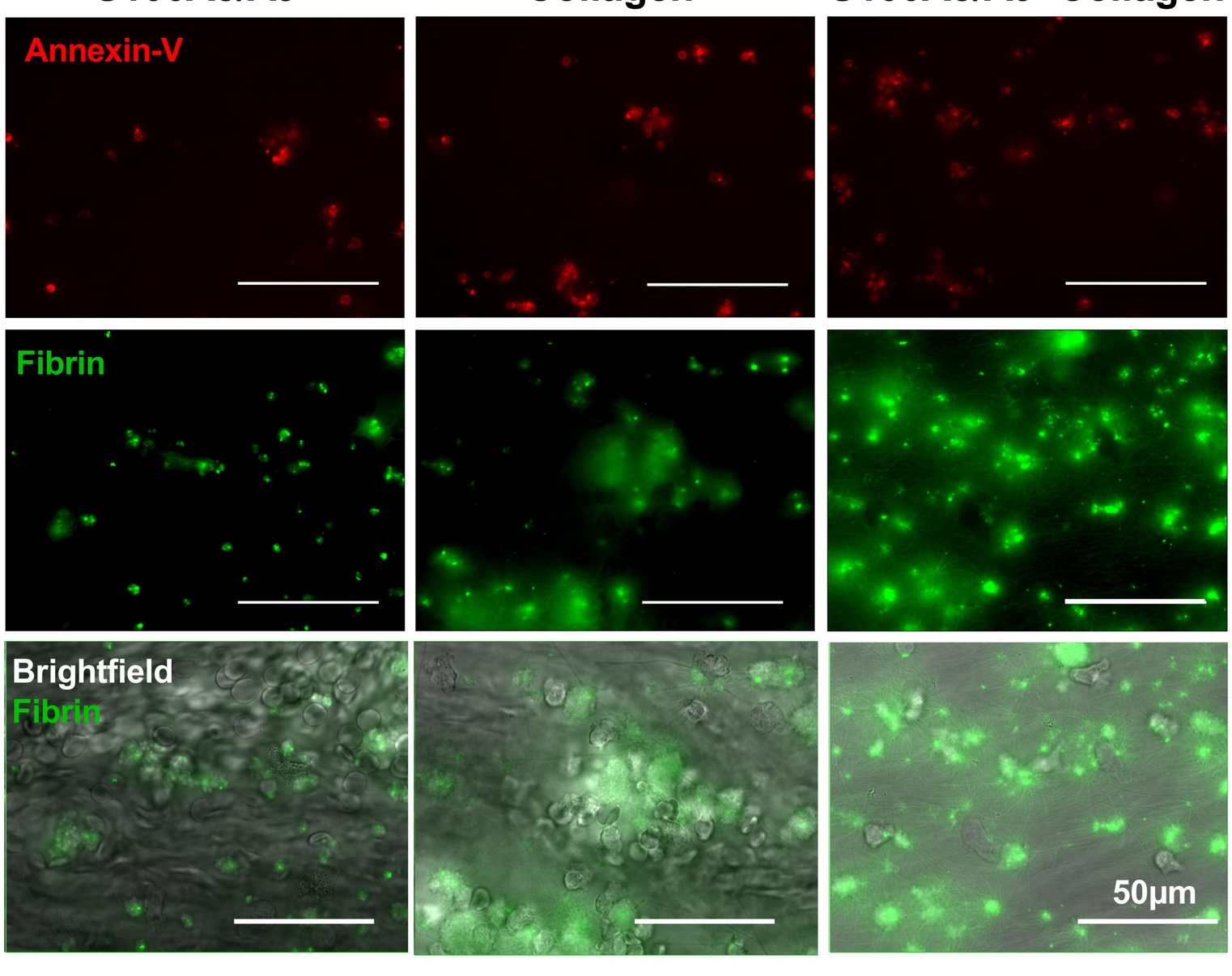


I

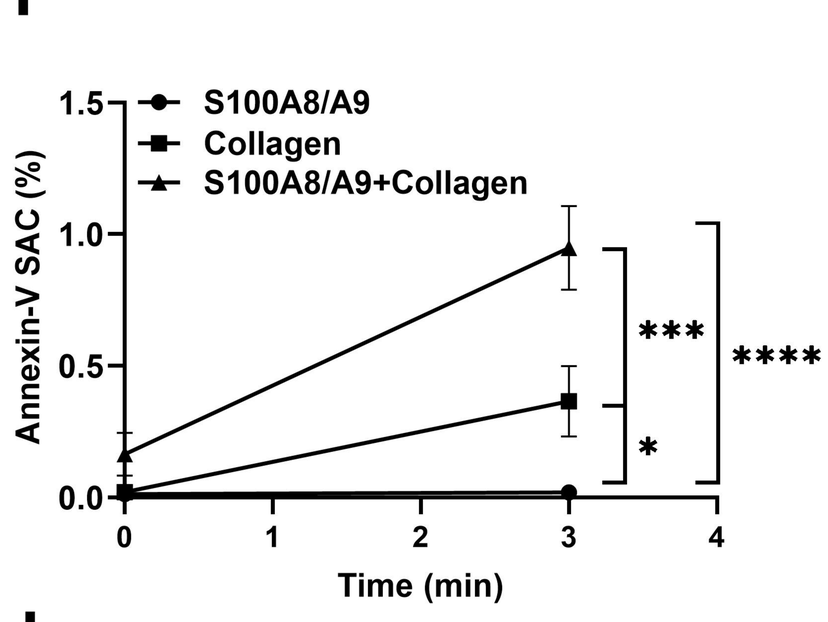


J

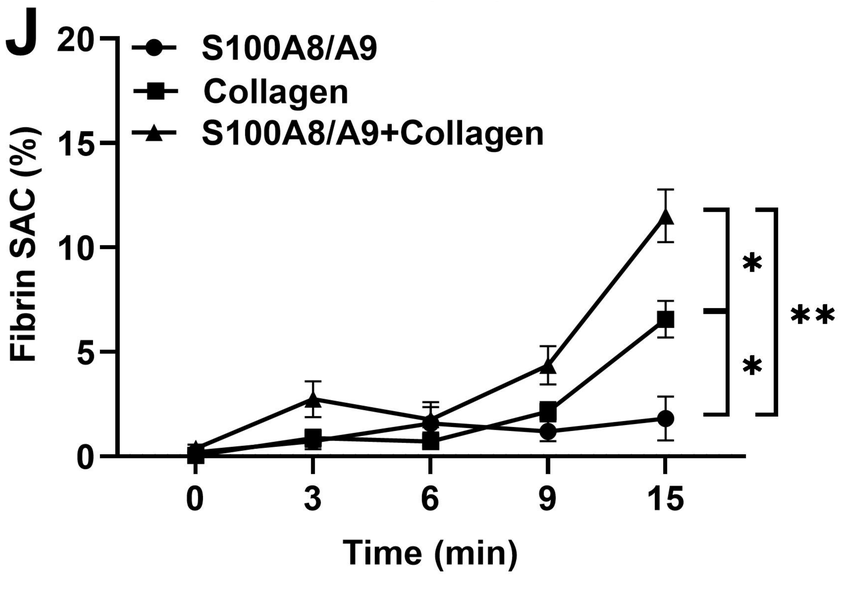

Figure 2

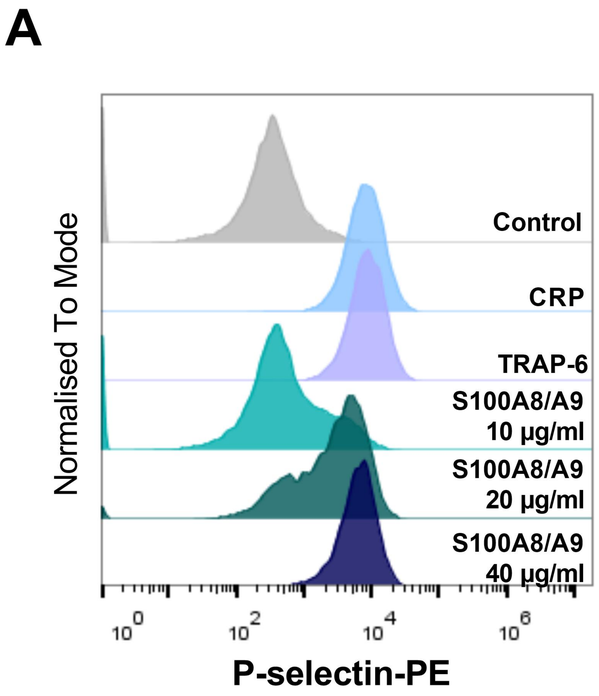
A
Normalised To Mode
Control
CRP
TRAP-6
S100A8/A9 10 µg/ml
S100A8/A9 20 µg/ml
S100A8/A9 40 µg/ml
P-selectin-PE

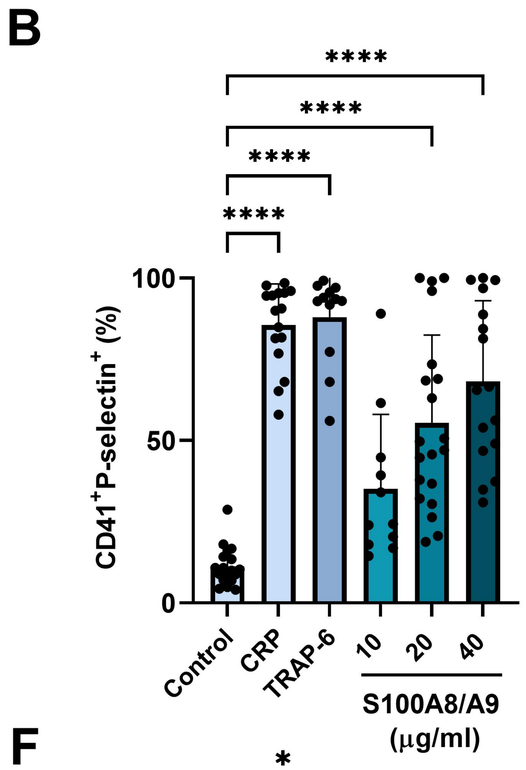
B
CD41+P-selectin+ (%)
Control
CRP
TRAP-6
S100A8/A9 (µg/ml)

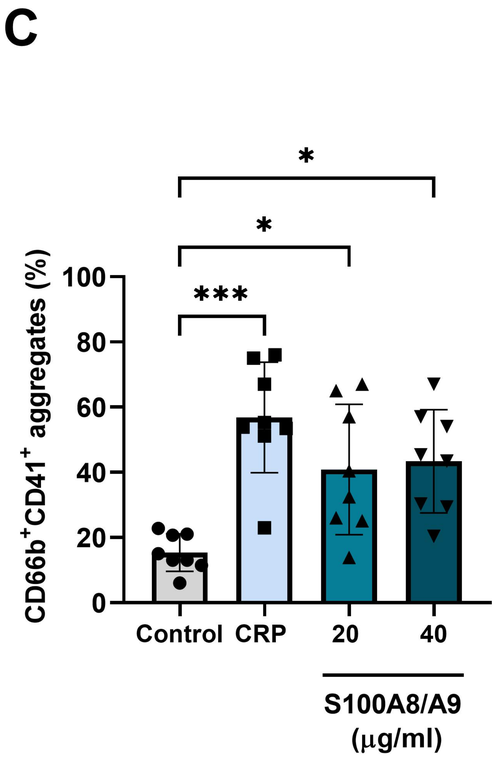
C
CD66b+CD41+ aggregates (%)
Control
CRP
S100A8/A9 (µg/ml)

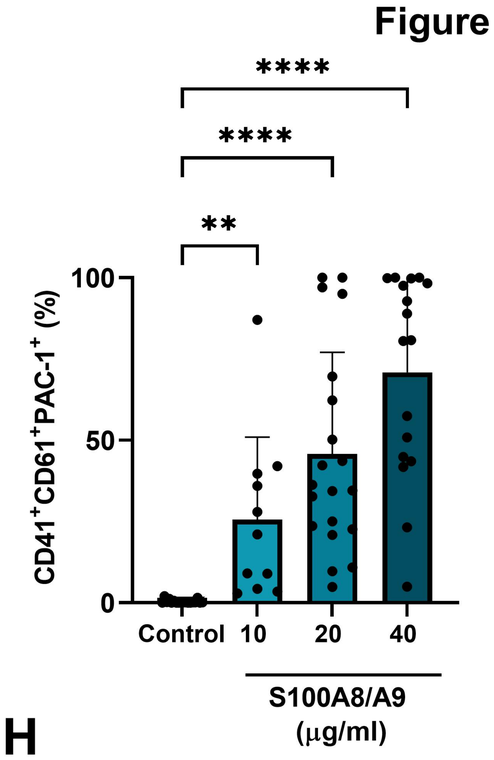
D
CD41+CD61+PAC-1+ (%)
Control
S100A8/A9 (µg/ml)

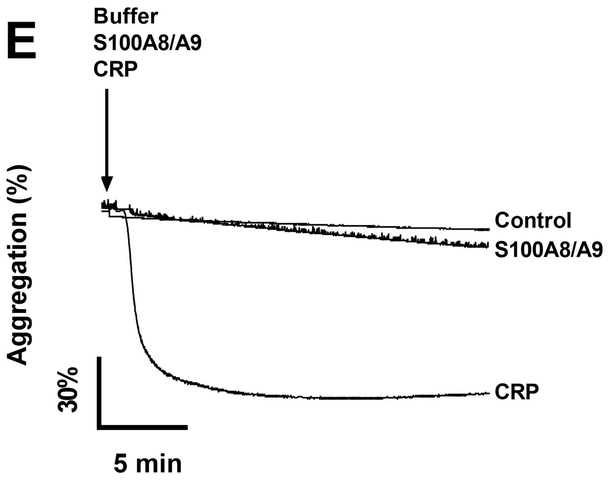
E
Buffer
S100A8/A9
CRP
Aggregation (%)
Control
S100A8/A9
CRP
30%
5 min

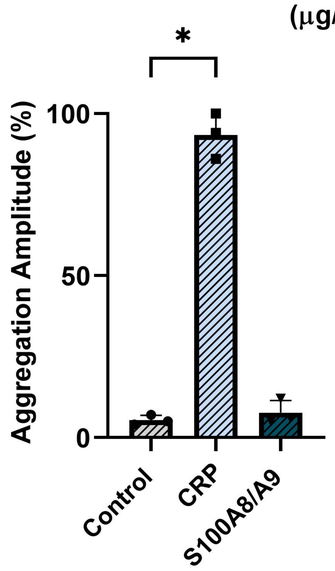
F
Aggregation Amplitude (%)
Control
CRP
S100A8/A9

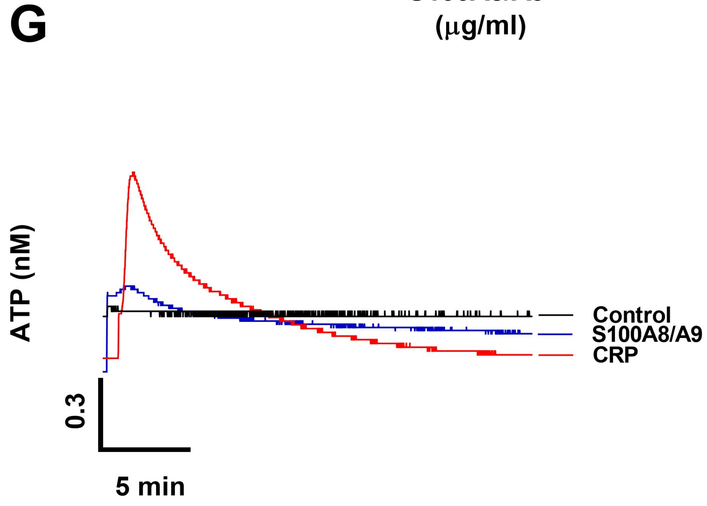
G
ATP (nM)
Control
S100A8/A9
CRP
0.3
5 min

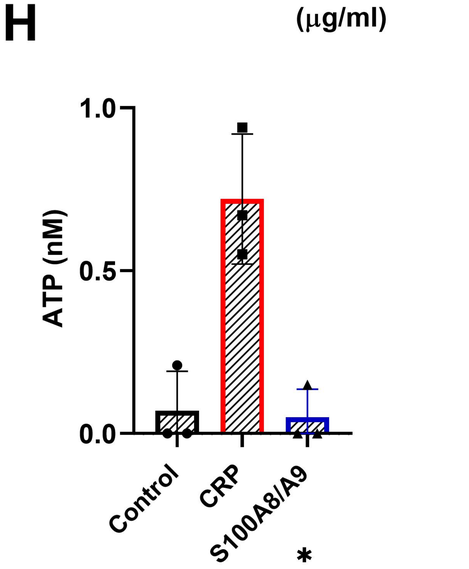
H
ATP (nM)
Control
CRP
S100A8/A9

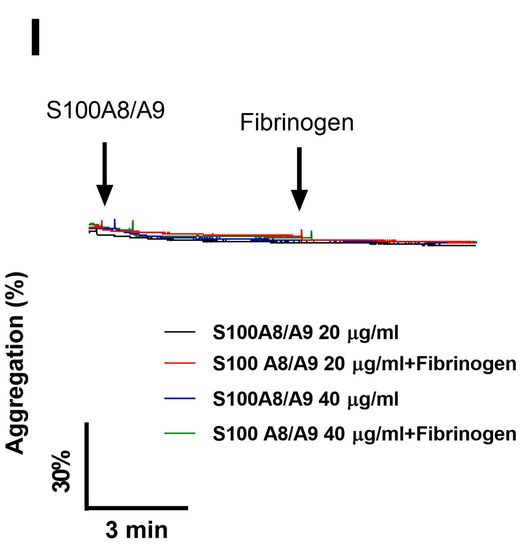
I
S100A8/A9
Fibrinogen
Aggregation (%)
S100A8/A9 20 µg/ml
S100 A8/A9 20 µg/ml+Fibrinogen
S100A8/A9 40 µg/ml
S100 A8/A9 40 µg/ml+Fibrinogen
30%
3 min

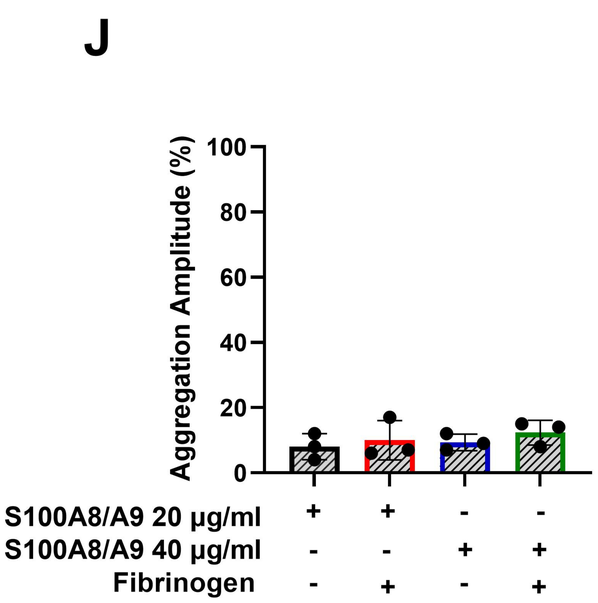
J
Aggregation Amplitude (%)
S100A8/A9 20 µg/ml
S100A8/A9 40 µg/ml
Fibrinogen

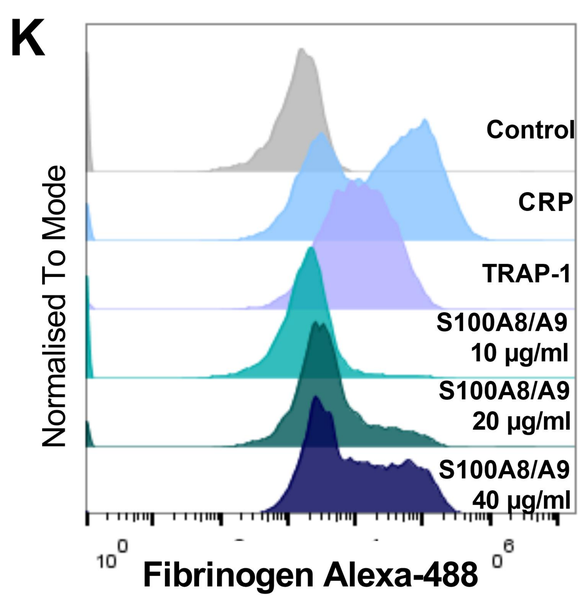
K
Normalised To Mode
Control
CRP
TRAP-1
S100A8/A9 10 µg/ml
S100A8/A9 20 µg/ml
S100A8/A9 40 µg/ml
Fibrinogen Alexa-488

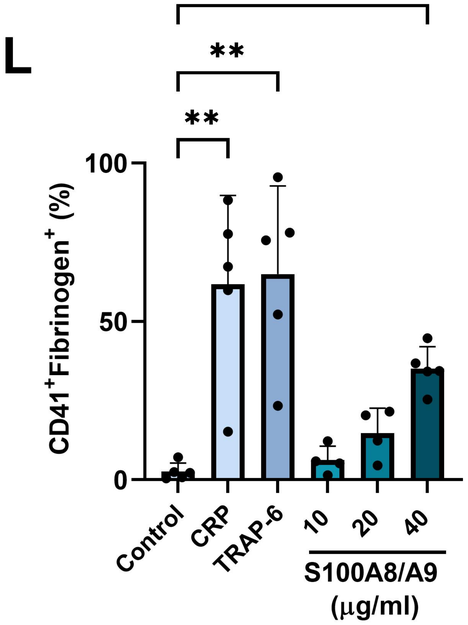
L
CD41+Fibrinogen+ (%)
Control
CRP
TRAP-6
S100A8/A9 (µg/ml)

Figure 3

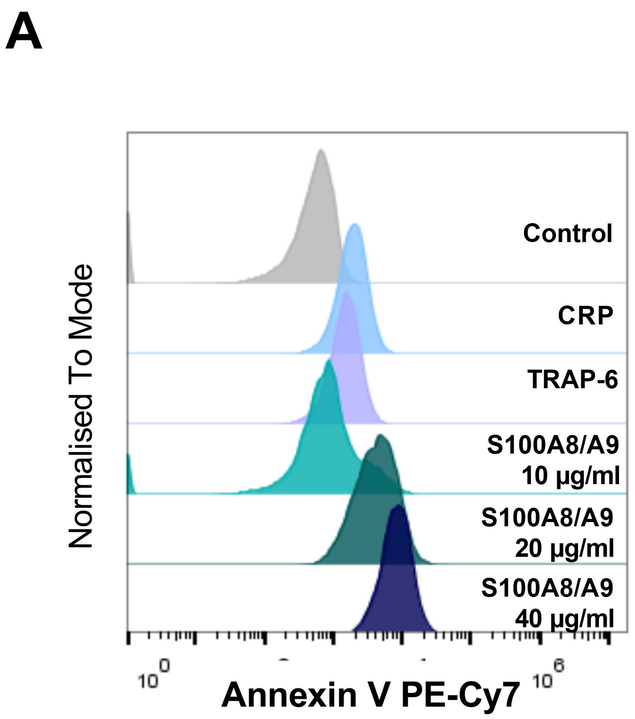
A
Normalised To Mode
Control
CRP
TRAP-6
S100A8/A9 10 µg/ml
S100A8/A9 20 µg/ml
S100A8/A9 40 µg/ml
Annexin V PE-Cy7

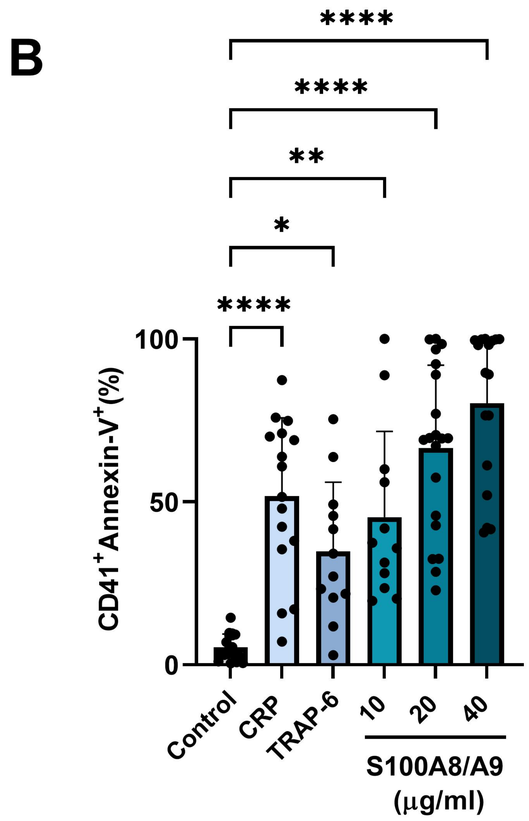
B
CD41+Annexin-V+(%)
Control
CRP
TRAP-6
10
20
40
S100A8/A9 (µg/ml)

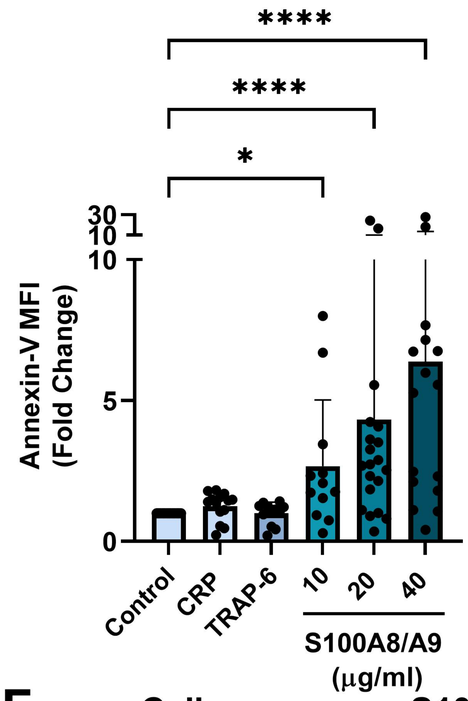
C
Annexin-V MFI (Fold Change)
Control
CRP
TRAP-6
10
20
40
S100A8/A9 (µg/ml)

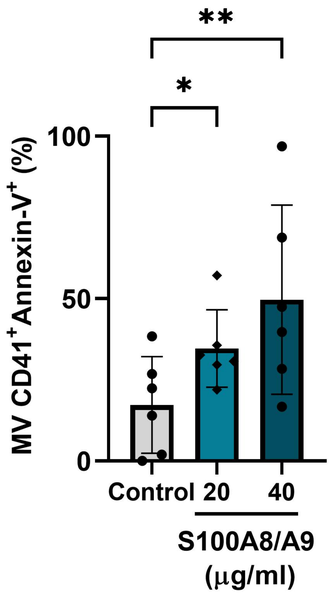
D
MV CD41+Annexin-V+ (%)
Control
20
40
S100A8/A9 (µg/ml)

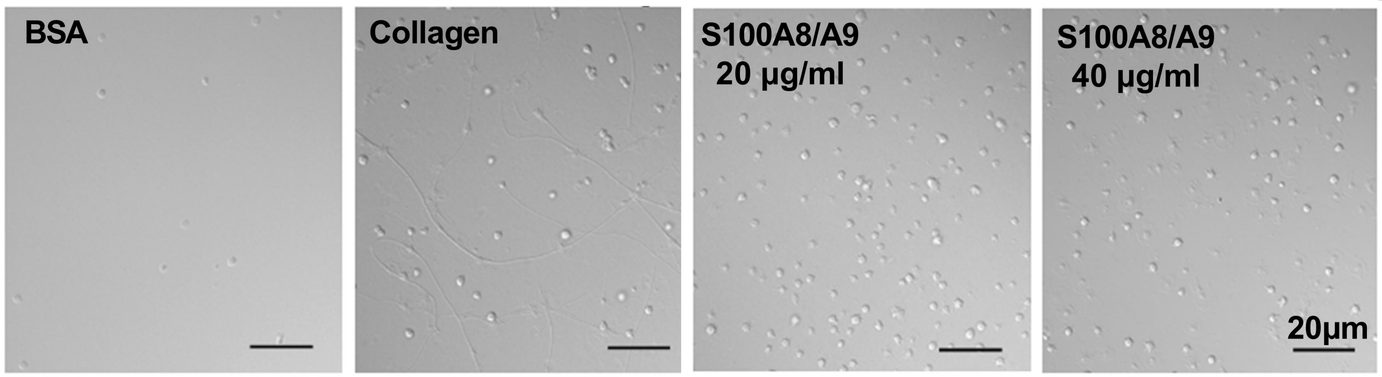
E
BSA
Collagen
S100A8/A9 20 µg/ml
S100A8/A9 40 µg/ml
20µm

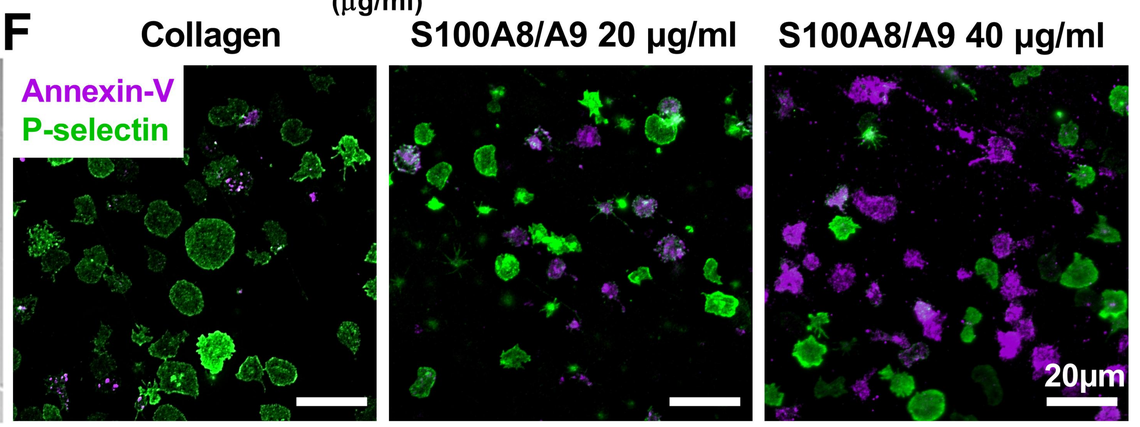
F
Collagen
S100A8/A9 20 µg/ml
S100A8/A9 40 µg/ml
Annexin-V
P-selectin
20µm

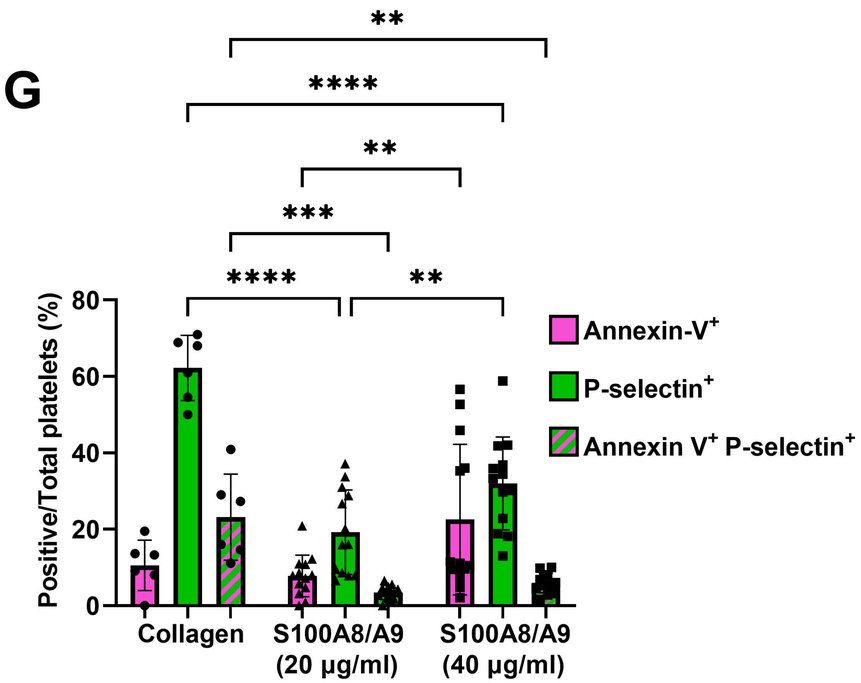
G
Positive/Total platelets (%)
Annexin-V+
P-selectin+
Annexin V+ P-selectin+
Collagen
S100A8/A9 (20 µg/ml)
S100A8/A9 (40 µg/ml)

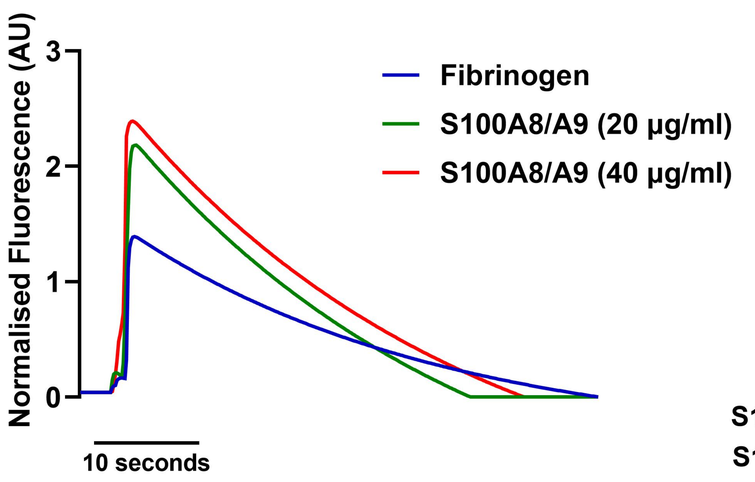
H
Normalised Fluorescence (AU)
Fibrinogen
S100A8/A9 (20 µg/ml)
S100A8/A9 (40 µg/ml)
10 seconds

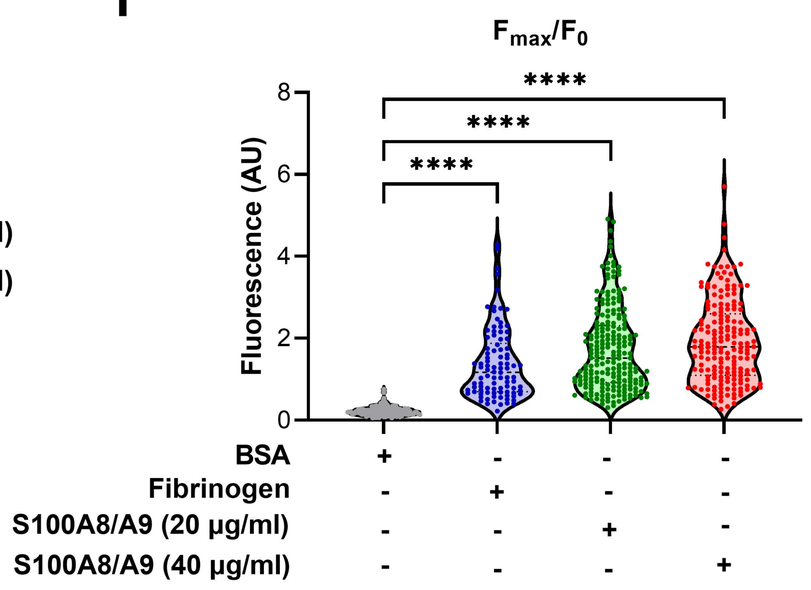
I
Fmax/F0
Fluorescence (AU)
BSA
Fibrinogen
S100A8/A9 (20 µg/ml)
S100A8/A9 (40 µg/ml)

Figure 4

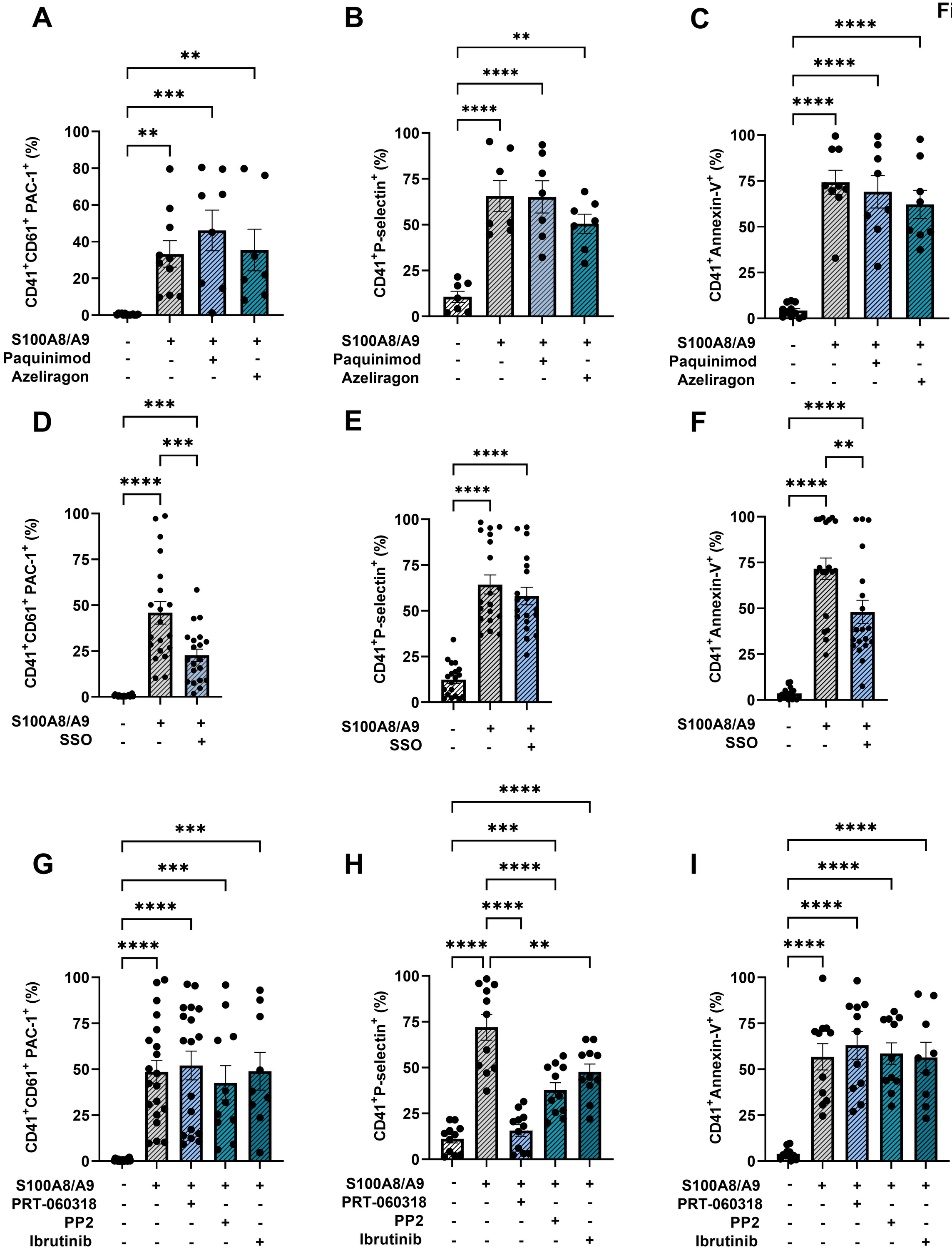
A
B
C
D
E
F
G
H
I
CD41+CD61+ PAC-1+ (%)
CD41+P-selectin+ (%)
CD41+Annexin-V+ (%)
S100A8/A9
Paquinimod
Azeliragon
SSO
PRT-060318
PP2
Ibrutinib

Figure 5

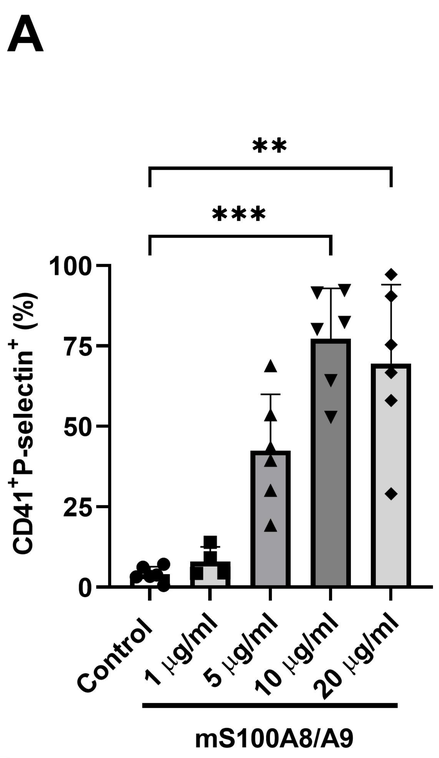
A
CD41+P-selectin+ (%)
Control
1 μg/ml
5 μg/ml
10 μg/ml
20 μg/ml
mS100A8/A9

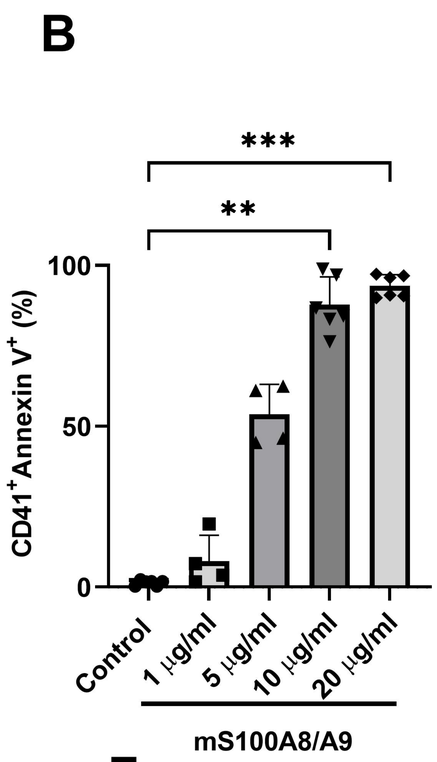
B
CD41+Annexin V+ (%)
Control
1 μg/ml
5 μg/ml
10 μg/ml
20 μg/ml
mS100A8/A9

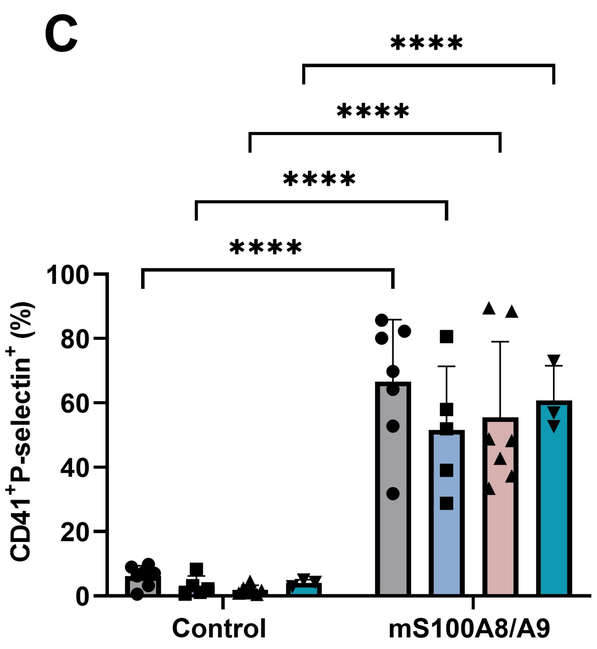
C
CD41+P-selectin+ (%)
Control
mS100A8/A9

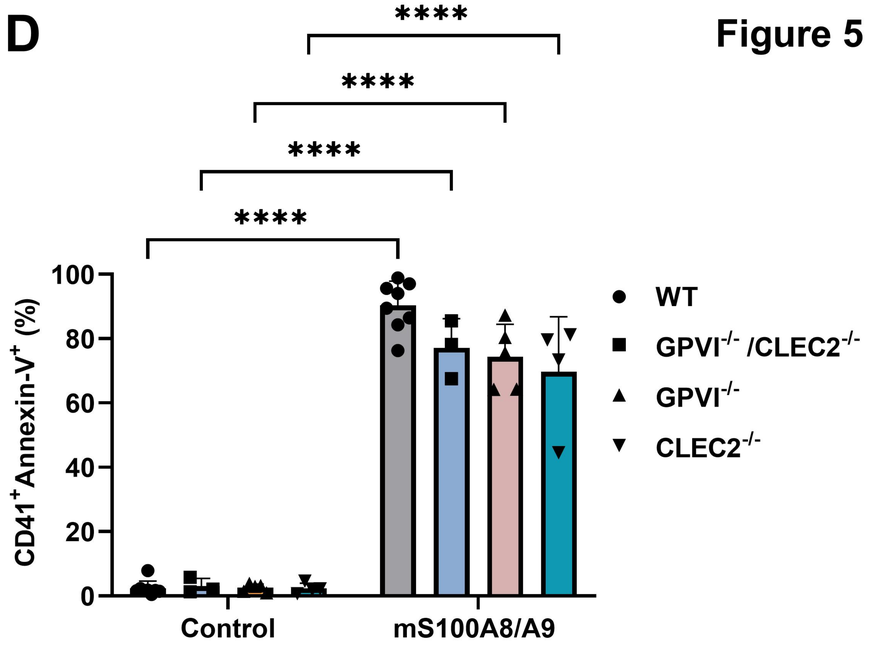
D
CD41+Annexin-V+ (%)
Control
mS100A8/A9
WT
GPVI-/- /CLEC2-/-
GPVI-/-
CLEC2-/-

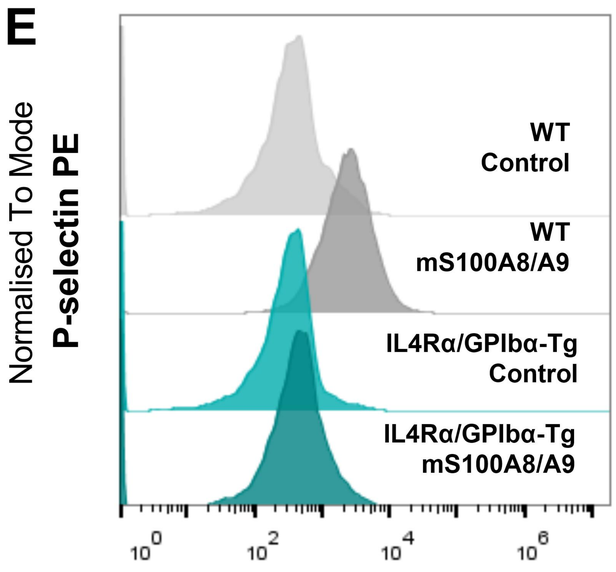
E
Normalised To Mode
P-selectin PE
WT Control
WT mS100A8/A9
IL4Rα/GPIbα-Tg Control
IL4Rα/GPIbα-Tg mS100A8/A9

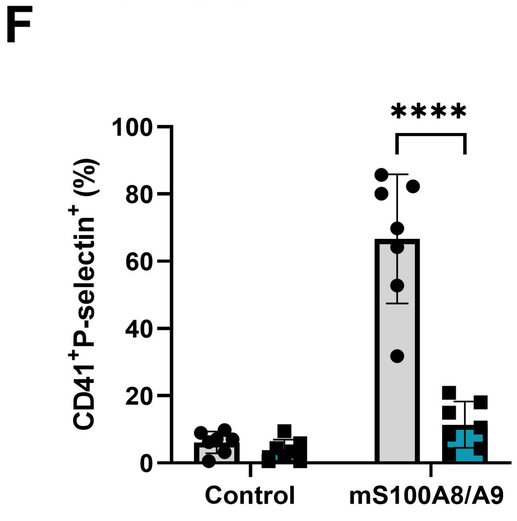
F
CD41+P-selectin+ (%)
Control
mS100A8/A9

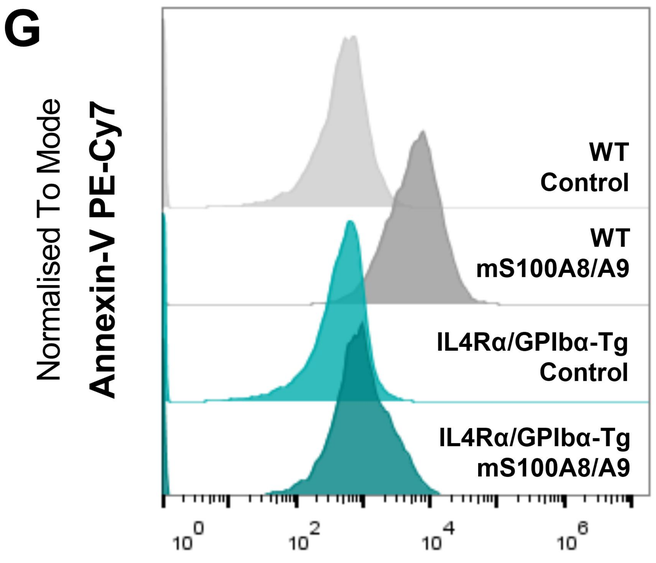
G
Normalised To Mode
Annexin-V PE-Cy7
WT Control
WT mS100A8/A9
IL4Rα/GPIbα-Tg Control
IL4Rα/GPIbα-Tg mS100A8/A9

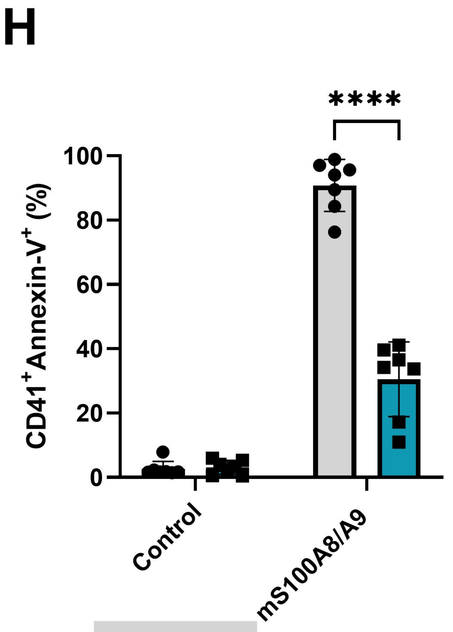
H
CD41+Annexin-V+ (%)
Control
mS100A8/A9
WT
IL4Rα/GPIbα-Tg

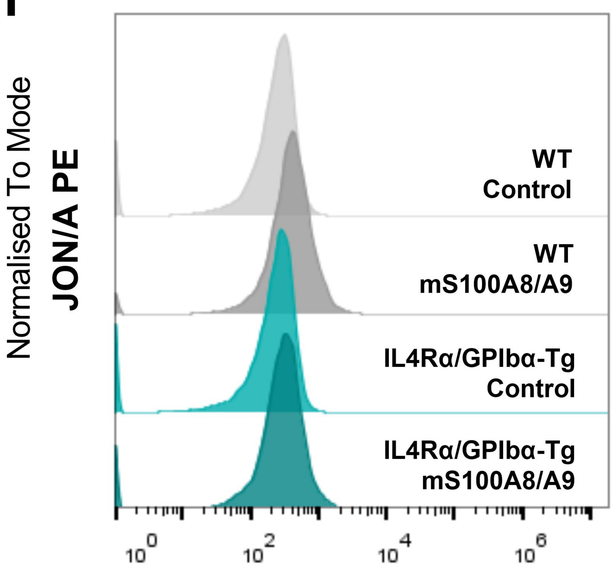
I
Normalised To Mode
JON/A PE
WT Control
WT mS100A8/A9
IL4Rα/GPIbα-Tg Control
IL4Rα/GPIbα-Tg mS100A8/A9

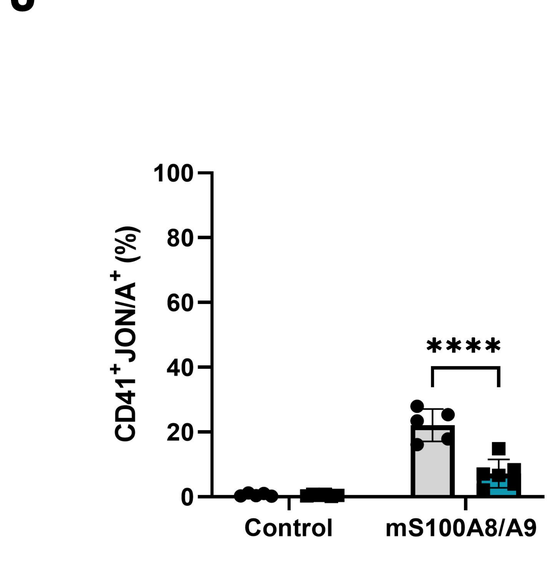
J
CD41+JON/A+ (%)
Control
mS100A8/A9

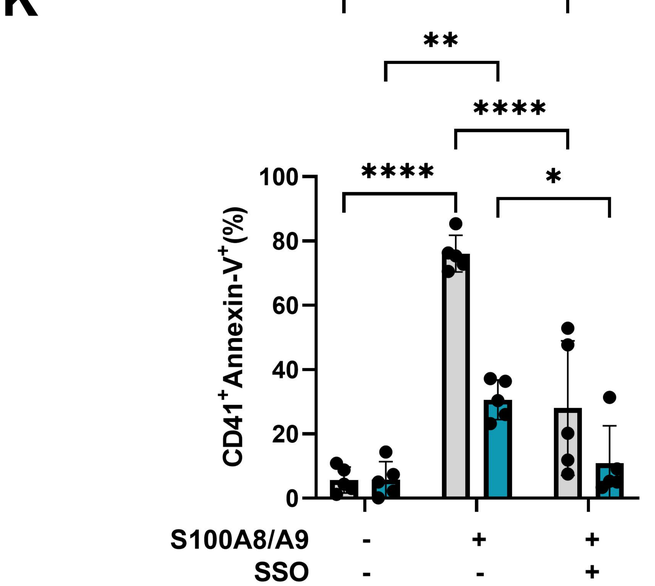
K
CD41+Annexin-V+(%)
S100A8/A9
SSO

Figure 6

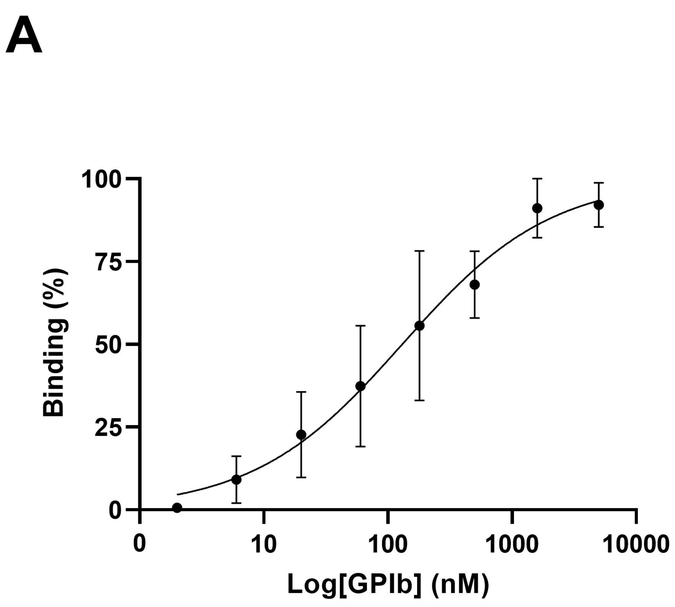
A
Binding (%)
100
75
50
25
0
0
10
100
1000
10000
Log[GPIb] (nM)

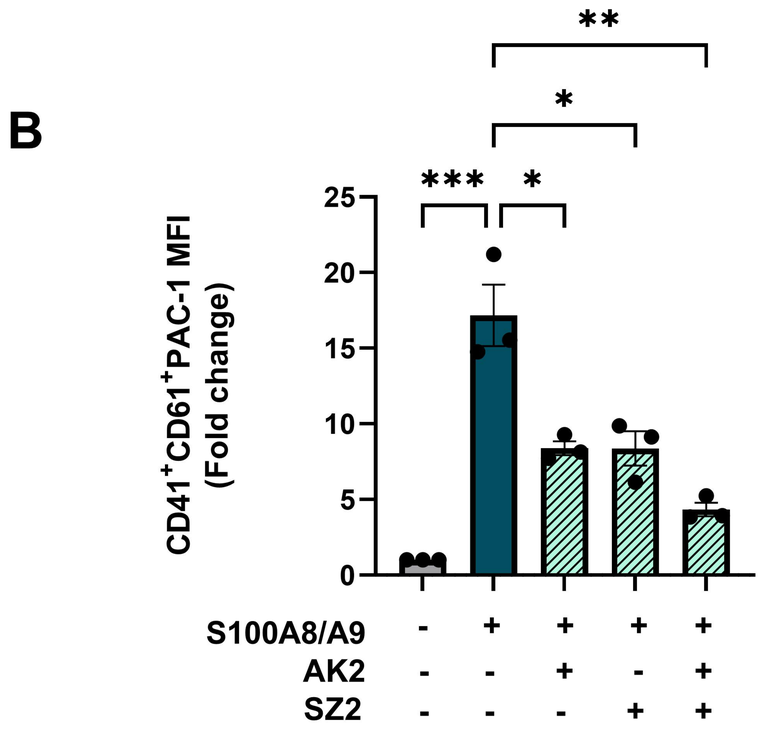
B
**
*
***
*
CD41+CD61+PAC-1 MFI
(Fold change)
25
20
15
10
5
0
S100A8/A9 - + + + +
AK2 - - + - +
SZ2 - - - + +

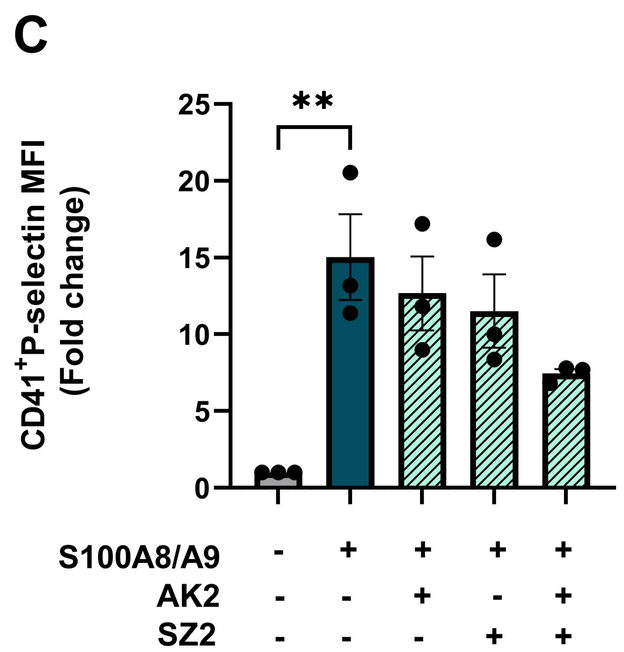
C
**
CD41+P-selectin MFI
(Fold change)
25
20
15
10
5
0
S100A8/A9 - + + + +
AK2 - - + - +
SZ2 - - - + +

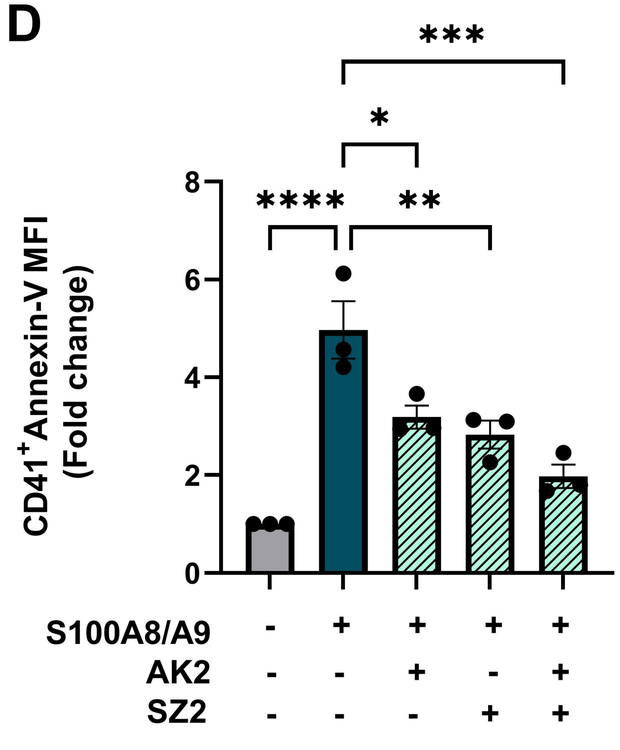
D
***
*
****
**
CD41+Annexin-V MFI
(Fold change)
8
6
4
2
0
S100A8/A9 - + + + +
AK2 - - + - +
SZ2 - - - + +

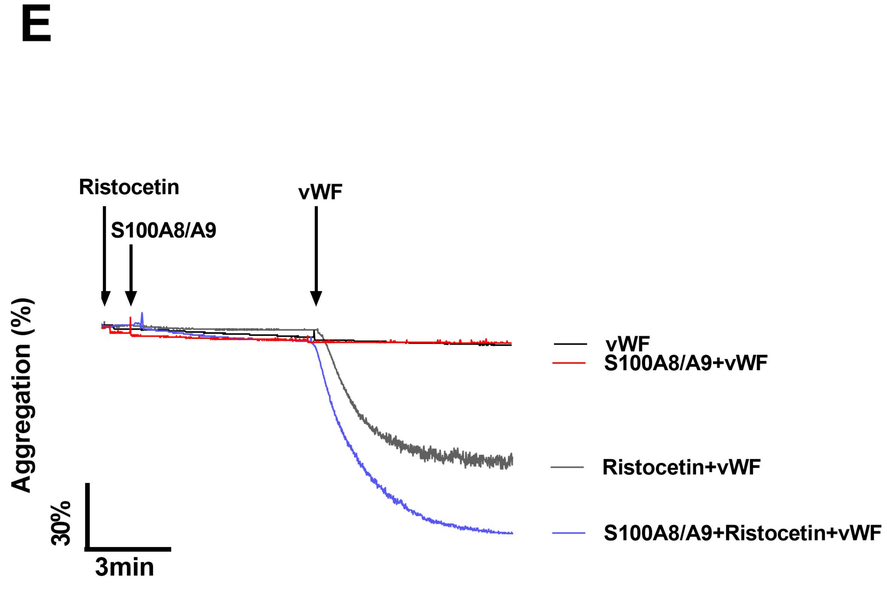
E
Ristocetin
S100A8/A9
vWF
Aggregation (%)
30%
3min
vWF
S100A8/A9+vWF
Ristocetin+vWF
S100A8/A9+Ristocetin+vWF

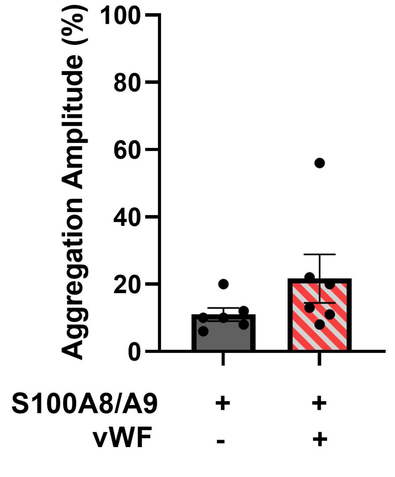
F
Aggregation Amplitude (%)
100
80
60
40
20
0
S100A8/A9 + +
vWF - +

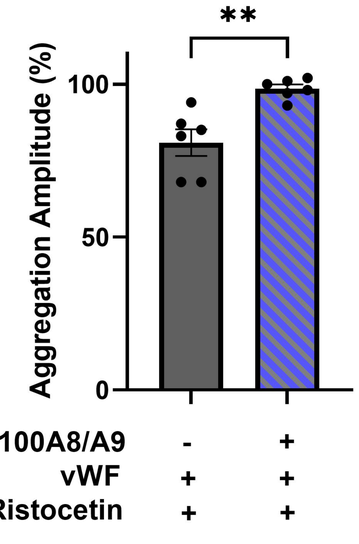
G
**
Aggregation Amplitude (%)
100
50
0
S100A8/A9 - +
vWF + +
Ristocetin + +

Figure 7

A

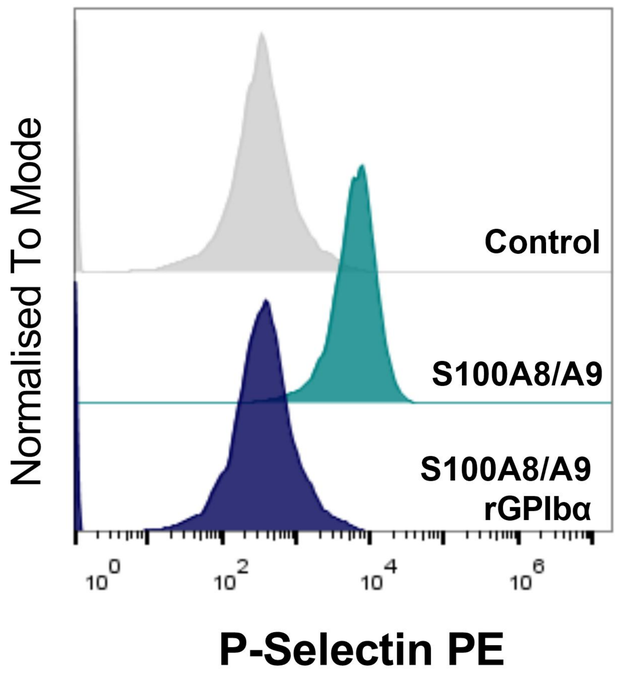


B

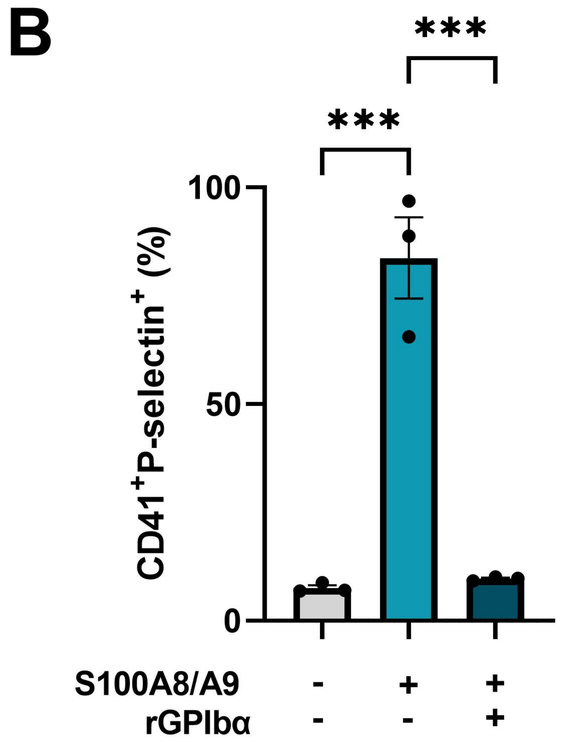


C

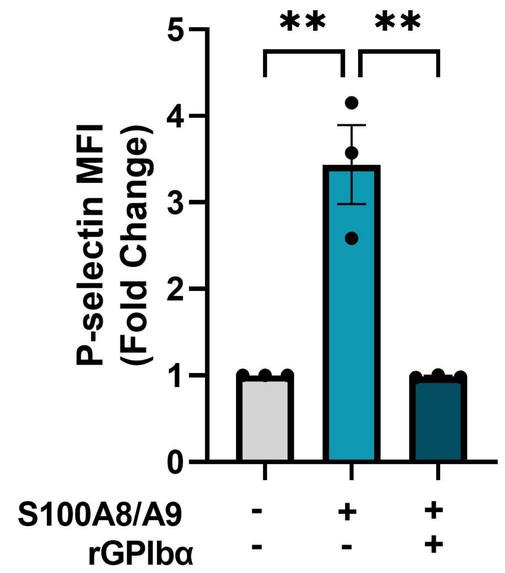


D

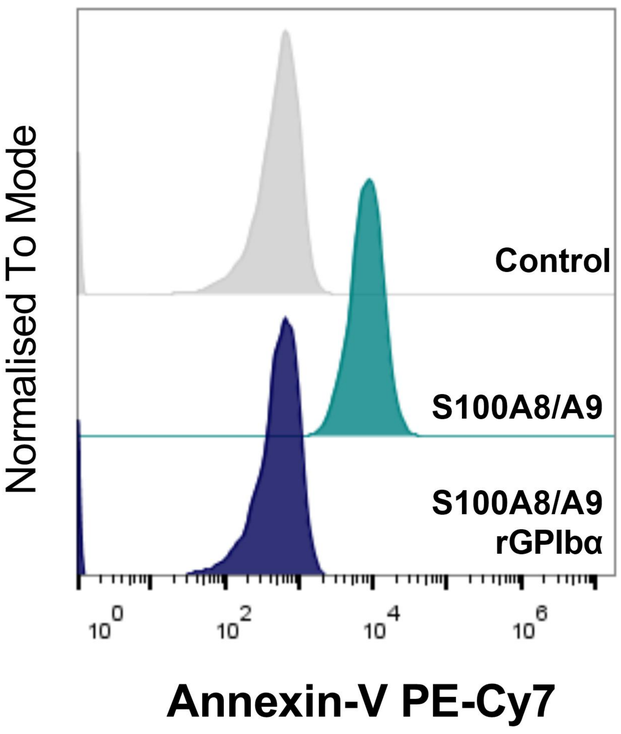


E

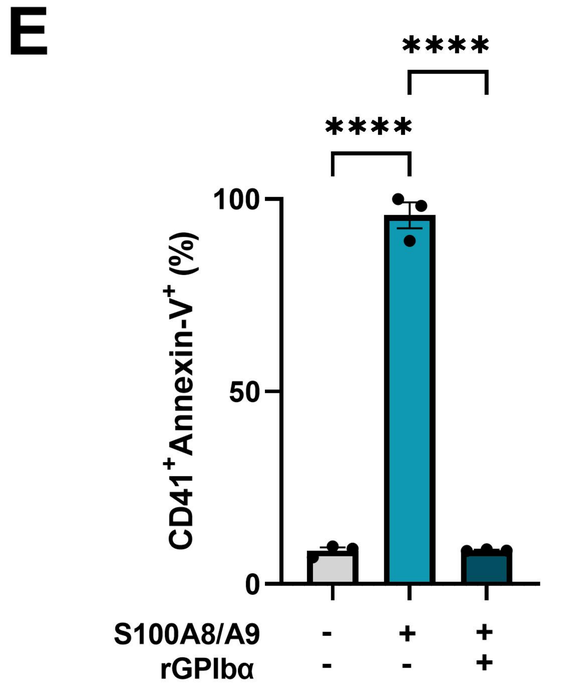


F

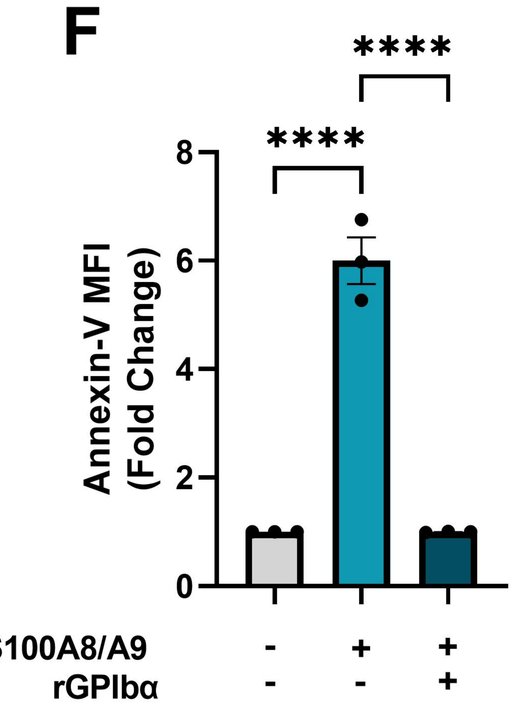


G

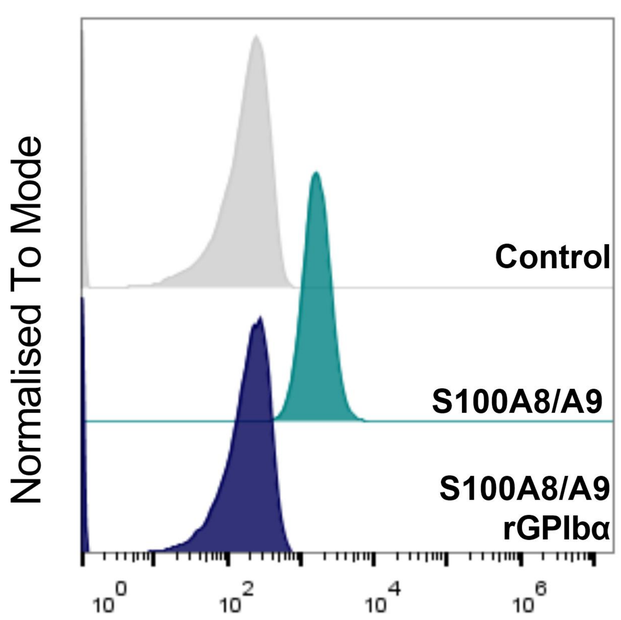


H

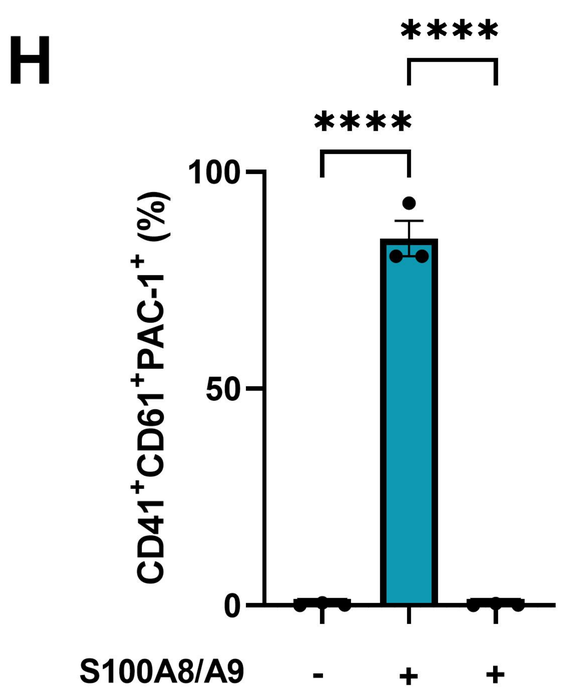


I

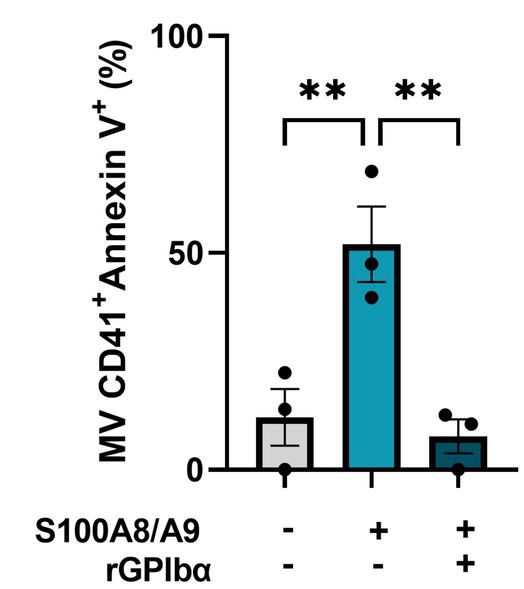


J

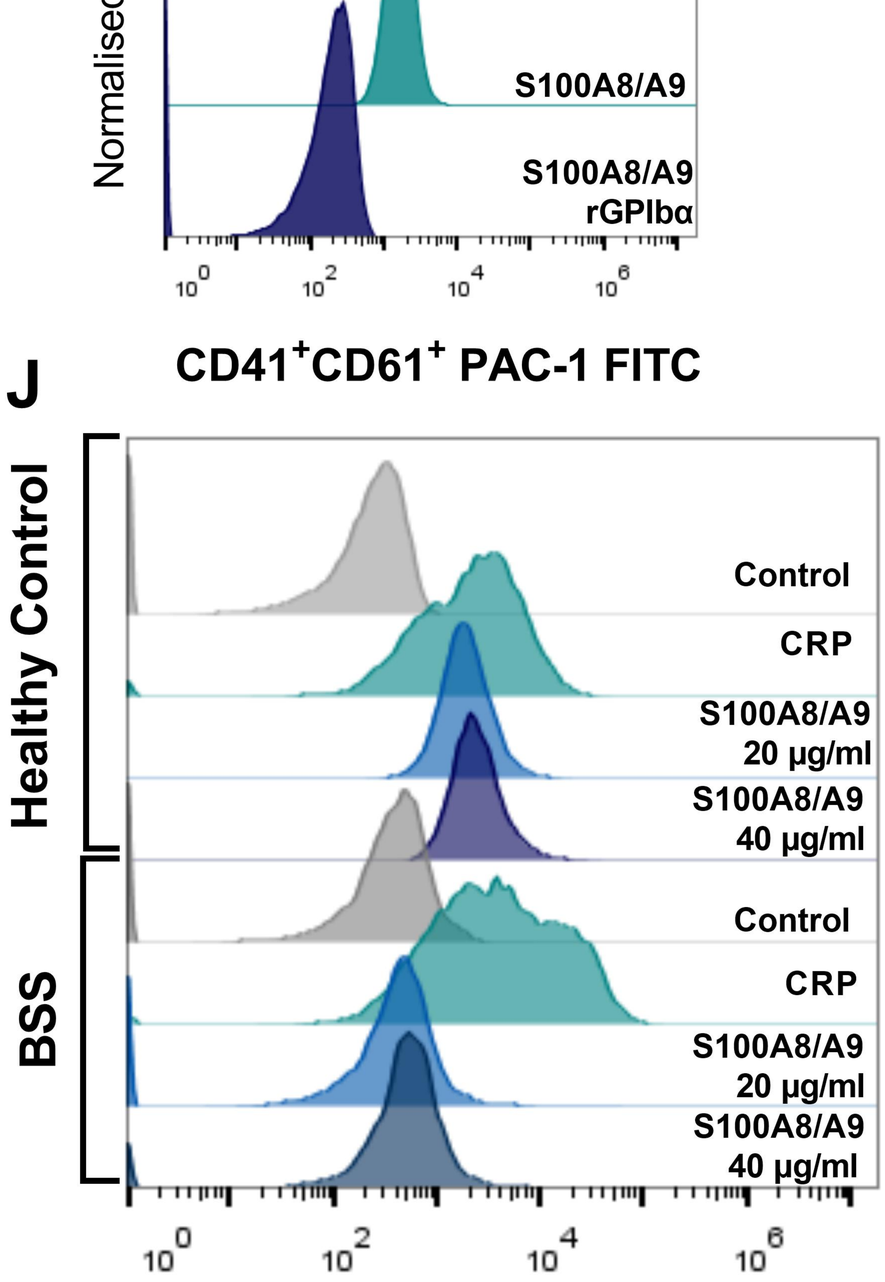


K

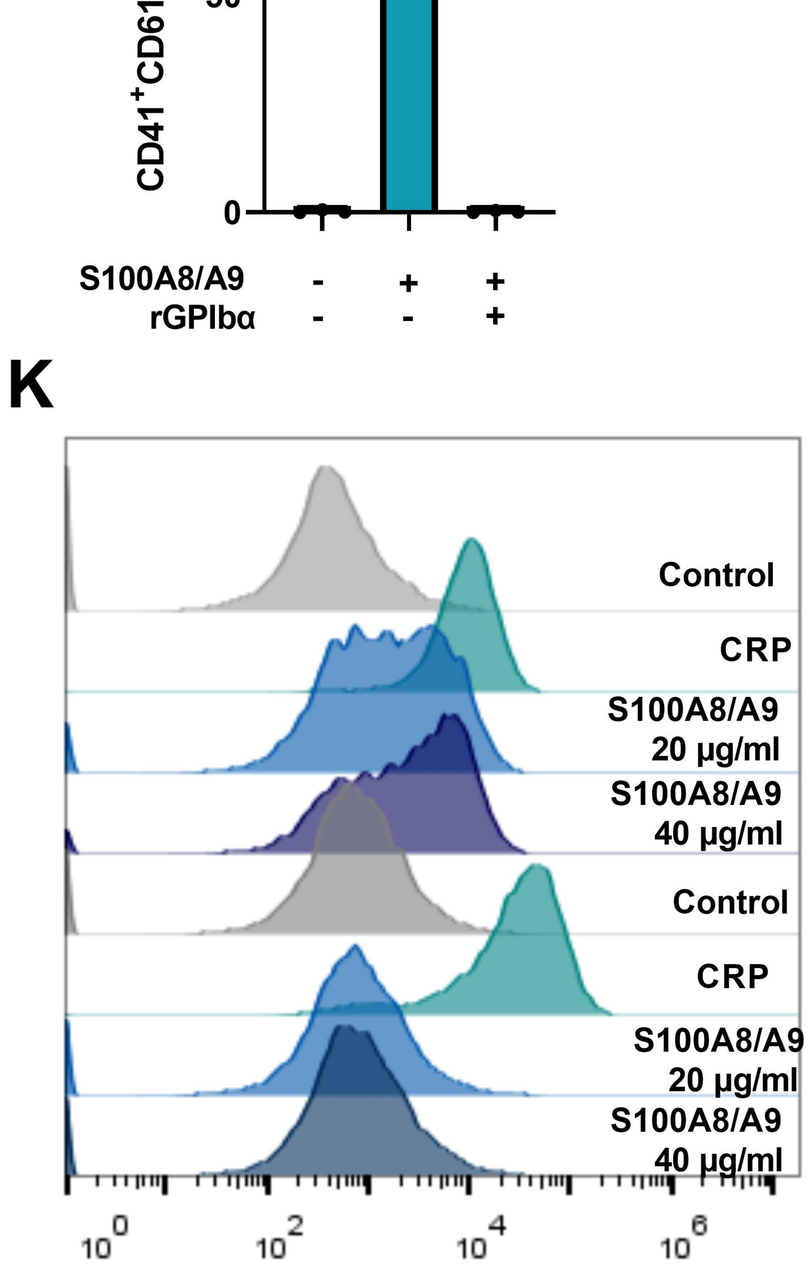


L